

2015•2016
FACULTEIT INDUSTRIËLE INGENIEURSWETENSCHAPPEN
*master in de industriële wetenschappen:
verpakkingstechnologie*

Masterproef

Fabrication and Characterization of Poly (L-lactic acid) Aluminum based
Metal Organic Frameworks Mixed Matrix Membranes

Promotor :
Prof. dr. ir. Mieke BUNTINX

Promotor :
Prof. dr. AJAY KATHURIA

Niels Brouwers

*Scriptie ingediend tot het behalen van de graad van master in de industriële
wetenschappen: verpakkingstechnologie*

Gezamenlijke opleiding Universiteit Hasselt en KU Leuven

2015•2016
Faculteit Industriële
ingenieurswetenschappen
*master in de industriële wetenschappen:
verpakkingstechnologie*

Masterproef

Fabrication and Characterization of Poly (L-lactic acid)
Aluminum based Metal Organic Frameworks Mixed Matrix
Membranes

Promotor :
Prof. dr. ir. Mieke BUNTINX

Promotor :
Prof. dr. AJAY KATHURIA

Niels Brouwers

*Scriptie ingediend tot het behalen van de graad van master in de industriële
wetenschappen: verpakkingstechnologie*

Acknowledgements

I would like to thank my supervisor prof. dr. ir. Mieke Buntinx for her guidance towards commencing my master's project at California Polytechnic State University. Without her contacts and direction, I would not have been able to study abroad.

I would also like to thank my project supervisor prof. dr. Ajay Kathuria who took me under his wing and shared his knowledge and experience and dr. Trevor Harding for his assistance during this project.

I am thankful for the faculty and staff of the California Polytechnic State University, San Luis Obispo, CA, for presenting the opportunity to work in such an ideal setting for my technical needs.

Finally, I want to thank my mother Brigitte Lacroix and her partner Marc Brosens, father Marc Brouwers for their support during this work. Without their financial support this work wouldn't be possible. More importantly, their unconditional belief and motivation inspired the confidence to complete this project with quality. Not only during the past 4 months, but for my entire life they have always believed in me. They have had a significant influence in the person I have become.

The topic of this project deepened my interest in biopolymers and their various applications. I strongly believe that they can play a more prominent role in the future.

I see this master thesis as the end of a great time as a college student, where I broadened my expertise as an engineer. I am truly blessed to have studied abroad in the United States, and will always remember this enlightening period.

I hope you will enjoy reading my thesis as much as I enjoyed the research.

Table of content

1	Introduction.....	15
1.1	Introduction.....	15
1.2	Goals and Objectives	17
1.3	Document Outline	17
2	Literature Review	19
2.1	Plastics.....	19
2.2	Biodegradable Polymers.....	19
2.3	Poly (lactic acid).....	21
2.3.1	Introduction.....	21
2.3.2	Structure and Synthesis of PLA.....	21
2.3.3	Applications	23
2.3.4	Commercialization and Numbers.....	23
2.3.5	Properties of PLA.....	24
2.3.6	Crystallinity.....	26
2.3.7	Comparison of Mechanical Properties of PLA to Other Polymers	27
2.3.8	PLA Blends	28
2.4	PLA Bio Composites.....	28
2.4.1	PLA/Natural filler Composites	28
2.4.2	PLA/Mineral Filler Composites	28
2.5	Nanocomposites.....	29
2.6	Porous Colloidal Articles.....	29
2.6.1	Adsorption/Adsorbents	29
2.6.2	Zeolites	30
2.6.3	Other Common Adsorbent Materials.....	30
2.7	Metal Organic Framework.....	31
2.7.1	Introduction.....	31
2.7.2	Application of Metal Organic Frameworks.....	32
2.7.3	Al - MOF.....	32
2.7.4	Mil-53 Series	32
2.7.5	Synthesis.....	33
2.8	Mixed Matrix Membranes (MMM)	33
2.8.1	Introduction.....	33
2.8.2	MMM Including MOF	33

2.9	PLA - MOF Mixed Matrix Membranes.....	34
2.10	Solvent Casting.....	34
3	Synthesis of PLLA - MOF MMMs.....	35
3.1	Introduction.....	35
3.2	Methodology.....	35
3.2.1	Materials.....	35
3.2.2	Sample Preparation.....	35
3.2.3	Compression Molding.....	36
4	Characterization of PLLA - MOF Composites.....	37
4.1	Fourier Transform Infrared Spectroscopy.....	37
4.2	Differential Scanning Calorimetry.....	37
4.3	Thermogravimetric analysis.....	37
4.4	Scanning Electron Microscopy.....	37
5	Results and Discussion.....	39
5.1	Fourier Transform Infrared Spectroscopy.....	39
5.2	Differential Scanning Calorimetry.....	43
5.3	Thermogravimetric Analysis.....	46
5.4	Scanning Electron Microscopy.....	48
6	Conclusion.....	51
7	Further Improvements.....	53
8	References.....	55

List of Tables

Table 1: Physical properties of PLA.	24
Table 2: Surface area of Basolite MOFs and other common used adsorbents.	31
Table 3: Wavenumbers (cm^{-1}) and vibrational assignments of neat PLLA.	40
Table 4: Wavenumbers (cm^{-1}) and vibrational assignments of Mil-53 (Al).....	41
Table 5: Area under peak 923 cm^{-1} related to the crystallinity of PLLA calculated by FTIR results.	42
Table 6: Thermal characteristics of neat PLLA and PLLA - MOF MMMs derived from DSC test.....	44
Table 7: TGA analysis of neat PLLA and PLLA - MOF MMMs.	47

List of Figures

Figure 1: Classification of the biodegradable polymers	20
Figure 2: chemical structure of L - Lactic acid and D - Lactic acid	21
Figure 3: Different synthesis methods for obtaining high molecular weight PLA	22
Figure 4: Oxygen permeability coefficient as a function of water activity for poly (98% L-Lactide)	26
Figure 5: Mechanical properties of PLA and other commodity plastics.	27
Figure 6: Structure of MIL-53 adapted from Yan et al.	32
Figure 7: Structure of A) 1,4-benzenedicarboxylic acid and B) Aluminum nitrate.....	33
Figure 8: Solvent casted PLLA-MOF samples after a total of 20 days.....	36
Figure 9: FTIR spectrum of neat PLLA.....	39
Figure 10: FTIR spectrum of MIL-53 (Al).....	40
Figure 11: FTIR spectrum of neat PLLA, AL - MOF and PLLA - MOF MMMs.....	41
Figure 12: FTIR spectra of neat PLLA and PLLA - MOF MMMs for the 1000 - 750 cm^{-1} region.....	42
Figure 13: DSC thermograms of neat PLLA and PLLA - MOF MMMs.	43
Figure 14: Crystallinity of neat PLLA and PLLA - MOF MMMs derived from DSC test.	45
Figure 15: TGA curves for PLLA and PLLA - MOF MMMs in the range of 50-600 $^{\circ}\text{C}$	46
Figure 16: SEM images of MOF and neat PLLA.	48
Figure 17: SEM images of PLLA - 1% MOF, PLLA - 5% MOF, PLLA - 10% MOF and PLLA - 20% MOF....	49

Key to symbols or abbreviations

Symbols	Key
DSC	Differential scanning calorimetry
FTIR	Fourier transformation infrared spectroscopy
MMMs	Mixed matrix membranes
MOF	Metal Organic Framework
PLLA	Poly (L-lactic acid)
SEM	Scanning electron microscopy
$T_{30\%}$	Temperature at 30% weight
$T_{50\%}$	Temperature at 50% weight
$T_{80\%}$	Temperature at 80% weight
T_{co}	Temperature of cold crystallization
T_g	Glass Transition Temperature
TGA	Thermogravimetric analysis
T_m	Melt Temperature
T_{max}	Temperature maximum decomposition
T_{onset}	Temperature of PLLA degradation
T_{vc}	Temperature of evaporation of volatile compounds
X_c	Crystallinity
wt%	Weight fraction
ΔH_c	Cold crystallization enthalpy
ΔH_m	Fusion enthalpy

Abstract

Poly (L-lactic acid) (PLLA) and Aluminum based Metal Organic Frameworks (MOFs) mixed matrix membranes (MMMs) were prepared by solvent casting PLLA with 1, 5, 10 and 20% w/w of MIL-53(Al). PLLA and PLLA-MOF MMMs were characterized by Fourier transform infrared spectroscopy (FTIR), scanning electron microscopy (SEM), differential scanning calorimetry (DSC) and thermal gravimetric analysis (TGA). DSC studies indicate that the addition of MOF particles in the PLA polymer matrix reduces the polymeric chain mobility, which affects the crystallization process. The percent crystallinity of neat PLLA was found to be 3.23% and decreased by around 4% for PLLA-1% MOF and 85% for PLLA-5% MOF as compared to neat PLLA. PLLA-10% MOF and PLLA-20% MOF compositions were completely amorphous. TGA results show that PLLA-MOF MMMs are thermally less stable than neat PLLA suggesting that MOF particles act as a depolymerization catalyst for PLLA. An average of 14% volatile compounds originated from trapped chloroform was found in neat PLLA and PLLA-MOF compounds. The variable wt% of MOF in the samples for the different PLLA-MOF ratios indicated that the MOF particles were not well dispersed in the PLLA matrix. This was confirmed by SEM analysis showing that MOF particles have the tendency to accumulate within the PLLA matrix. In this study non-homogeneous MMMs containing chloroform were fabricated. Future work can be focused on improving the synthesis technique and the impact of MOF particles on permeability of PLLA-MOF MMMs for different compounds.

Abstract in Dutch

Poly (L-melkzuur) (PLLA) en aluminium gebaseerde *Metal Organic Frameworks* (MOFs) mixed matrix membranen (MMMs) werden gemaakt via solvent casting met 1, 5, 10 and 20% w/w MIL-53 (Al) en de eigenschappen van PLLA versus PLLA–MOF MMMs werden geëvalueerd door differentiële scanning calorimetrie (DSC), Fourier transform infrarood spectroscopie (FTIR), scanning elektronen microscopie (SEM) en thermogravimetriscche analyse (TGA). DSC resultaten tonen aan dat toevoeging van MOF-deeltjes in de PLLA-polymeer matrix de mobiliteit van de polymeerketens vermindert. De kristalliniteit van zuiver PLLA bedroeg 3.23% en verminderde met 4% voor PLLA-1%MOF en met 85% voor PLLA-10%MOF in vergelijking met zuiver PLLA. PLLA-10%MOF en PLLA-20%MOF vertonen geen kristalliniteit. TGA resultaten tonen aan dat PLLA-MOF MMMs minder thermisch stabiel zijn dan zuiver PLLA. Dit doet vermoeden dat MOF-deeltjes zich gedragen als een depolymerisatie katalysator voor PLLA. Een gemiddelde van 14% vluchtige stoffen bestaande uit chloroform was geobserveerd voor zuiver PLLA en de PLLA-MOF MMMs. Het uiteenlopend gewichtspercentage van MOF in de stalen voor de verschillende PLLA-MOF verhoudingen suggereerde dat de MOF deeltjes niet goed verdeeld waren in de PLLA matrix en werd bevestigd in de SEM-analyse. In deze studie werden niet homogene MMMs gemaakt die chloroform bevatten. Toekomstig onderzoek kan zich focussen op het verbeteren van de synthesesetchniek en op de impact van MOF-deeltjes op de permeabiliteit van PLA-MOF MMMs voor verschillende stoffen.

1 Introduction

1.1 Introduction

Petroleum based polymers such as polyethylene (PE), polypropylene (PP), polyethylene terephthalate (PET), polystyrene (PS), and polyvinyl chloride (PVC) have been widely used for common packaging applications, due to their desired properties and commercial viability. Some of these features performance factors include good tensile and tear strength, good barrier to oxygen, carbon dioxide, water and aroma compounds. [1] They have the advantage to reduce food waste by extending their shelf life and improving transportation efficiency. Despite these noticeable advantages over other packaging material types, petroleum based polymers must be weighed against the problem that its durability and incredible volume worldwide constitute a waste stream. Packaging plastic waste possesses namely serious ecological problems and created increasing concerns over the last few years for manufacturers and the public in general. [2] To find more environmentally friendly packaging alternatives and improving product and packaging design to use less plastic, the use of bioplastics should be the future. [3, 4] In the last decade, new bio packaging materials produced from renewable and non-renewable resources e.g. poly(butylene-co-adipate-terephthalate) (PBAT) and poly(ϵ -caprolactone) (PCL) are being developed and studied due to their recovering ability through biodegradation and/or composting under specific conditions, leaving carbon dioxide, humus, and water as by-products. [3] Poly (lactic acid) (PLA), a highly versatile, biodegradable polymer derived from lactic acid, is proving to be a viable alternative to petrochemical-based plastics. It is produced from renewable resources such as corn and sugar beets, and is biodegradable, decomposing into H₂O, CO₂, and humus. PLA is not a new material since it was developed in 1932 by Carothers and offers great promise in a wide range of commodity applications although the commercial viability has historically been limited by its high production costs. [3, 5-7] PLA was first used in biomedical applications, and currently it is also widely used in packaging applications such as films, thermoformed cups and clamshells, and bottles. [3] PLA is due to its excellent barrier to flavor and aroma compounds and selective barrier properties the most common used biopolymer for fresh food packaging. It has been affirmed that PLA is safe and generally recognized as safe (GRAS) for its use in food-contact articles and that it can be suitable for the same food applications as synthetic polymers like PET, PS, etc. However, there are certain limitations on the use of PLA for food packaging. The most important limitation on the use of PLA for food application packaging is the medium barrier to gases and vapors and the brittleness properties. Therefore, modification of the biodegradable polymer through innovative technology has already proven to be an effective way to improve these properties concurrently. A possible solution therefore is the use of blends between PLA and other polymers or even nanocomposites. Already existing developments such as modified atmosphere packaging (MAP) and active packaging provide active or selective barrier properties during product shelf-life. Another way to manage this limitation involves incorporating a functional membrane into the packaging structure itself with achieving a more uniform scavenging effect throughout the packaging. [3] Mixed Matrix Membranes (MMM) can be described as a homogeneous dispersion of filler particles in a polymeric matrix. [8, 9] It's morphology and separation performance depends both on the polymer and filler properties. The presence of various mesoporous or microporous fillers such as zeolites and carbon molecular sieves prove to have an increasing permeability effect and enhance the separation properties of MMM. Unfortunately, matrix sub-micron size holes can come into play due to the poor compatibility between the inorganic fillers and organic polymer making these MMM not as effective as expected for gas separation applications. [10, 11]

The newest interest goes therefore to metal organic framework (MOF) particles due to their strong interfacial interactions between MOF and the polymer and their good thermal stability. [12] Metal Organic Frameworks (MOFs) are a class of crystalline compounds composed of metal ions linked together by organic bridging ligands forming one-, two-; or three-dimensional porous structures. [3, 8] These sophisticated nanostructured materials have high porosity, ultrahigh surface areas, large pore sizes and micro-pore volume making them a promising candidate for high capacity adsorption of various gases and molecules. [8] MOF applications include gas purification, gas separation, and heterogeneous catalysis. [3] Different MOF properties and structures can be achieved based on the selected metal and linker. For example, the geometry of the pores and the number of ligands that bound to the metal and orientation depends on the coordination preference of different metals. [3] Sadakiyo *et al.* [13] confirmed that the framework flexibility around the central metals of MOFs is related to the selective adsorption behavior. By selecting the appropriate building blocks and/or by post-synthetic modification their chemical environment can be adjusted. [9] Guest molecules can diffuse into the MOFs bulk structure while the size, shape and affinity of these pores provide selectivity among the guests. Their surface area is close to one order of magnitude higher than that of activated carbon and zeolites, namely between 1000 and 3000 m²/g or more. Many researchers have investigated the use of MOF particles in poly (lactic acid) by fabricating mixed matrix membranes to tailor the permeability of various gases, water molecules and organic compounds for various industrial applications such as gas separation and packaging. Kathuria *et al.* [12] studied the effect of Cu₃(BTC)₂ MOF in PLLA matrix on different gases (CO₂, O₂), H₂O and organic aroma compounds (trans-2-hexenal, acetaldehyde) by mass transfer and perm-selectivity. Results showed that addition of 20% (w/w) Cu₃(BTC)₂ MOF increased the carbon dioxide and trans-2-hexenal permeability. This was due to strong physisorption type interaction between the gas molecules and the MOF unlike the aromatic or water molecules who did not show any changes in the mass transfer properties. [12] It was also observed that [14] toughness of the PLLA - Cu₃(BTC)₂ MOF composites improved compared to neat PLLA. SEM and rheological studies indicated that the cavitation induced by debonding at the interface of PLLA and Cu₃(BTC)₂ MOF particles caused these improving toughness of the composites during uniaxial stress tests. MIL-53 series are a special class of MOF materials with 1-D diamond shaped pores with a free diameter of 8.6 Å build from MO₄(OH)₂ octahedra (M referring to Fe³⁺, Cr³⁺, Al³⁺, Ga³⁺, In³⁺ or Sc³⁺) and 1,4-benzenedicarboxylate (terephthalate) linkers. Many researchers focused their attention on it due to its high thermal and chemical stability and the ability to reversibly change their framework when guest molecules are introduced. [15] This phenomenon, also called the breathing effect allows the pores to reversibly contract or open upon adsorption of molecules. [9] MIL-53 Aluminum exhibits extraordinary thermal stability up to 450 °C and its members reversibly uptake/release water. The high hydrothermal stability is due to the strong Al-O bonds and octahedral coordination of aluminum. The surpass in stability towards water prolongs their lifetime, rendering their wide-ranging use economically more worthwhile. [16] The purpose of this research is therefore to explore the possible use of MIL-53 Aluminum as a filler in a PLA matrix by fabricating mixed matrix membranes to overcome the low barrier properties of PLA. This will hopefully encourage the global utilization of PLA in various applications, including packaging.

1.2 Goals and Objectives

The main goal of this research is to produce PLLA - Mil-53 (Al) MOF based functional mixed matrix membranes. In this paper the characterization of the membranes will be described. The new PLLA-MOF functional membranes are expected to have a good interaction with each other, and better permeability properties what will hopefully enhance the use of PLA MMMs in different sorts of applications. MOF's open internal structures, long-range crystallinity and distinctive pore sizes can accommodate different types of gases such as CO₂, O₂, N₂, CH₄ and volatile organic compounds (VOCs). [3] This could be useful in gas separation or packaging applications to selectively purge molecules that are considered unwanted in packaging because they can affect the quality of the product or the perception of the customer. [8]

In summary, the objectives of this master's thesis are:

1. Fabrication of poly (lactic acid) (PLA) biopolymer composites with different Aluminum Metal Organic Frameworks ratio (PLLA, PLLA-1% MOF, PLLA-5% MOF, PLLA-10% and PLLA-20% MOF) by solvent casting.
2. Compression molding the samples in order to produce thin PLA-MOF films to execute the permeability test.
3. Characterization of PLLA and PLLA - MIL-53 MOF composites evaluated by differential Scanning Calorimeter (DSC), Fourier Transform Infrared Spectroscopy (FTIR) and scanning electron microscopy (SEM).
4. Investigation of the thermal properties by thermal gravimetric analysis (TGA).

1.3 Document Outline

The thesis is divided into 5 different sections, consisting of the following topics:

1. Chapter 1 contains the introduction
2. Chapter 2 gives a literature review about biopolymers and more specifically about PLA, MOF particles and mixed matrix membranes.
3. Chapter 3 provides the methodology and preparation for the synthesis of the different PLA - MOF MMMs.
4. Chapter 4 describes the characterization of PLA - MOF MMMs using DSC, FTIR, TGA and SEM analysis.
5. Chapter 5 shows the obtained results and discussion for neat PLLA and PLLA - MOF MMMs.
6. Chapter 6 gives a general conclusion about the obtained results.
7. Chapter 7 describes an outlook to further improvements.

2 Literature Review

2.1 Plastics

In the world as we know it, petroleum based polymers such as polyethylene (PE), polypropylene (PP) and polyethylene terephthalate (PET) have provided most of common packaging materials, due to their desired features. Some of these features are lower cost, higher performance factors like good tensile and tear strength, good barrier to oxygen, carbon dioxide, water and aroma compounds. [1] They have the advantage to reduce food waste by extending their shelf life and improving transportation efficiency. The study of polymeric materials can be divided into three different divisions for their applications in packaging and other related fields: 1) conventional, 2) partially degradable, and 3) completely biodegradable polymers. [3] Most of the conventional, general petroleum-based, plastics have an impenetrable matrix which makes them not biodegradable due to the microorganisms that are not able to consume portions of the plastic. [17] The second examined division of polymeric materials, produced from petroleum or biomass resources, is partially degradable and designed with the goal of faster degradation in contrast to the conventional plastics. The microbes partly digest the macromolecules in the polymer matrix after the product is disposed and the weakened material undergoes further degradation until it is completely degraded. The final type are polymers, obtained from petroleum and/or renewable resources, that are biodegradable and/or compostable. [3]

2.2 Biodegradable Polymers

Despite the noticeable advantages over other packaging material types, petroleum based polymers must be balanced against the problem that its durability and incredible volume worldwide constitute a waste stream. Packaging plastic waste possesses namely serious ecological problems and created increasing concerns over the last few years for manufacturers and the public in general. [2] To find more environmentally friendly packaging alternatives and improving product and packaging design to use less plastic, the use of bioplastics should be the future. [3, 4] In the hope that they become cost- and performance-wise competitive with oil-based polymers. [18] In the last decade, new packaging produced from renewable and non-renewable resources e.g. PBAT and PCL are being developed and studied due to their recovering ability through biodegradation and/or composting under specific conditions, leaving carbon dioxide, humus, and water as by-products.[3] Fig.1 illustrates the classification of biodegradable polymers (biopolymers) in four different categories, depending on the synthesis: (a) polymers made out of biomass products from agro-resources such as polysaccharides (e.g. starch and cellulose) and proteins; (b) polymers obtained by extraction from micro-organisms such as polyhydroxyalkanoates (PHA); (c) polymers that are chemically synthesized by the use of monomers obtained from biotechnology such as PLA; (d) polymers whose monomers and polymers are both achieved by chemical synthesis from petrochemical products. Only categories (a)-(c) are obtained from renewable resources and are called the agro-polymers. The category's (b)-(d) are named biodegradable polyesters (bio polyesters). [19]

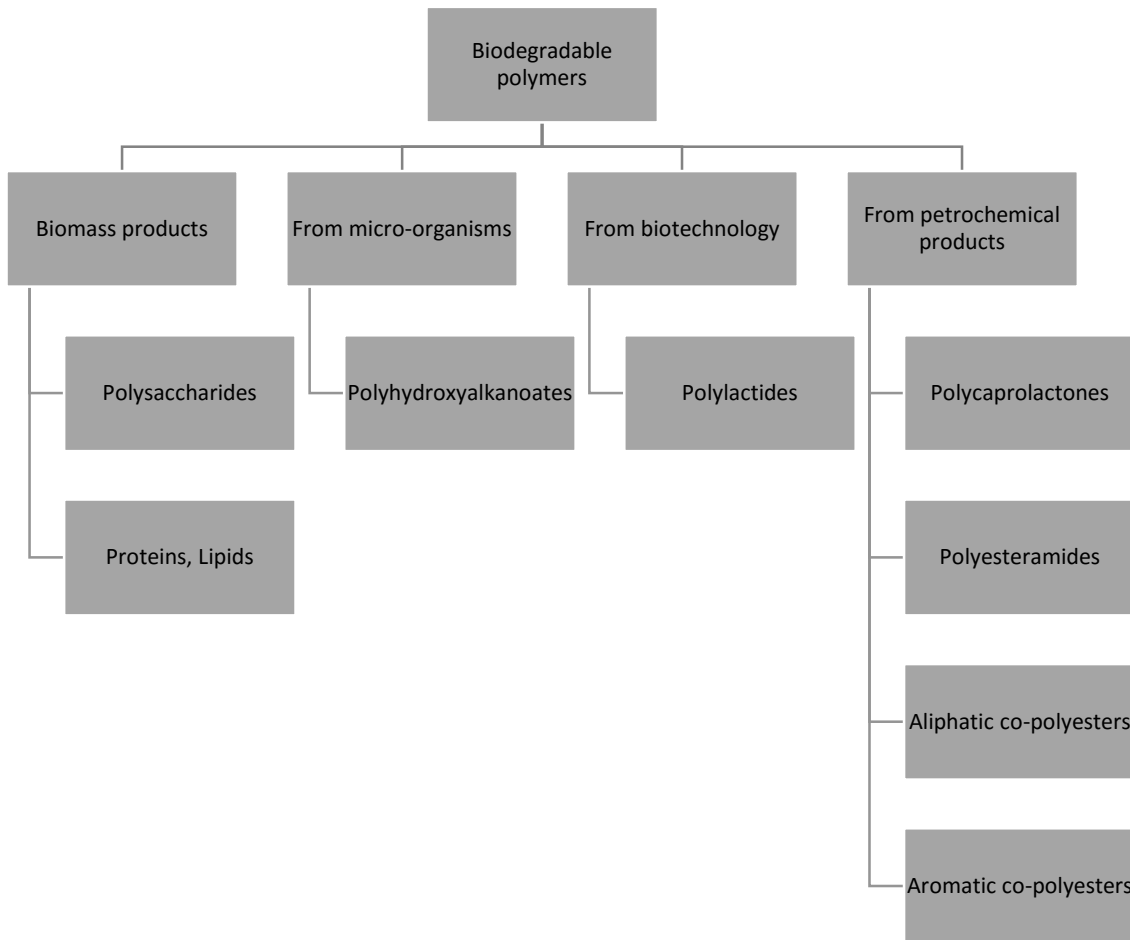


Figure 1: Classification of the biodegradable polymers. [19]

Bioplastics have already found large applications such as collection bags for compost, agricultural foils, etc. Also in the field of medicine, for example PLA has been used in biomedical applications. Other fields such as food packaging and technical application are gaining interest. Due to its higher cost, biopolymers were not taken into consideration for other applications which have already cheaper options available with conventional plastics. Thanks to the awareness of environmental pollution and the higher production volumes of these polymers in the recent years, the cost and the challenges of performance are being solved. Many of these biodegradable polymers, such as PLA, poly(-3-hydroxybutyrate) (PHB), aliphatic aromatic co polyesters like PBAT and poly (tetra methylene adipate-co-terephthalate) (PTAT), PCL and cellulose based polymers are entering the field of packaging. [1, 3] It is important to control and modify the mechanical and barrier properties of the bioplastic materials used in food packaging applications to contain the food, protecting it from the environment and maintaining food quality. Furthermore, it is important to study the compatibility with the food that can occur during interaction. [20] One of the most promising biopolymers is PLA, which is widely used in packaging applications such as films, thermoformed cups and clamshells, and bottles. [3]

2.3 Poly (lactic acid)

2.3.1 Introduction

The front-runner in the emerging bioplastics market is PLA, a highly versatile, biodegradable polymer derived from lactic acid, with the best availability and most attractive cost structure. [18] PLA is proving to be a viable alternative to petrochemical-based plastics. It is produced from renewable resources such as corn and sugar beets, and is biodegradable, decomposing to give H₂O, CO₂, and humus. It's a thermoplastic polymer with similar rigidity and clarity properties as polystyrene (PS) or poly (ethylene terephthalate) (PET). [21] PLA has a degradation time in the range of 6 months to 2 years, which is fast comparing to petrol based polymers like PS and PET who have a degradation time between 500 and 1000 years. [22] PLA is not a new material since it was developed in 1932 by Carothers and offers great promise in a wide range of commodity applications although the commercial viability has historically been limited by its high production costs. [3, 5-7] PLA was first used in biomedical applications, and currently it is also widely used in packaging applications such as films, thermoformed cups and clamshells, and bottles. [3] PLA is due to its excellent barrier to flavor and aroma compounds and selective barrier properties the most common used biopolymer for fresh food packaging. It has been affirmed that PLA is safe and generally recognized as safe for its use in food-contact articles and that it can be suitable for the same food applications as synthetic polymers like PET, PS, etc. However, there are certain limitations on the use of PLA for food packaging. The most important limitation on the use of PLA for food application packaging is the medium barrier to gases and vapors and the brittleness properties. [3]

2.3.2 Structure and Synthesis of PLA

The fabrication of the aliphatic polyester from lactic acid is comparatively straightforward. The basic constitutional unit of PLA, lactic acid (2-hydroxy propionic acid), a naturally occurring acid and bulk produced food additive for example as a buffering or acidic flavoring agent, is the simplest hydroxyl acid with an asymmetric carbon atom. [22] It exists in two optically active configurations, the L(+) and D(-) isomers as shown in Figure 2 and can be manufactured by carbohydrate fermentation or chemical synthesis. Purification of lactic acid is therefore of decisive importance otherwise there could be impurities such as acids, alcohols etc. containing the crude lactic acid. The majority of lactic acid is made by bacterial fermentation of carbohydrates and mainly under anaerobic conditions due to the more favorable oxidation of a sugar to carbon dioxide and water. [18] Microorganisms mainly produce lactic acid to keep the cellular processes going and generally L-lactic acid is produced, and no major sources of D-lactic acid are available, although some lactobacilli are reported to produce D-lactic acid. The fermentation can be classified according to the type of the bacteria used, namely the heterofermentative and homofermentative method. The homofermentative pathways are mainly used by industry due to the greater yields of lactic acid and lower levels of byproducts. In general, sources of simple sugars such as glucose and maltose from corn or potato, sucrose from cane or beet sugar and lactose from cheese whey are used. [6, 18, 22]

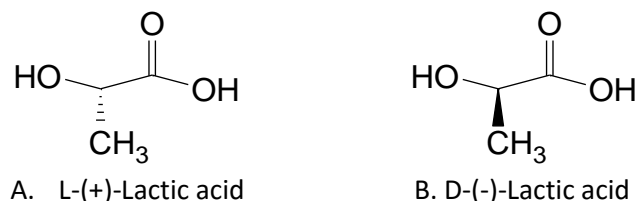


Figure 2: chemical structure of L - Lactic acid and D - Lactic acid. [6]

High molecular weight PLA can be obtained by 3 different routes (see Figure 3).

- 1) Direct condensation polymerization is an equilibrium reaction, but difficulties removing trace amounts of water in the late stages of polymerization generally limit the ultimate molecular weight achievable by this approach. It is necessary to adjust chain coupling agents and adjuvants for obtaining a solvent-free high molecular weight PLA which adds cost and complexity to the process.
- 2) Azeotropic dehydrative condensation of lactic acid yield high molecular weight PLA by the use of a catalyst along with diphenyl ester.
- 3) Polymerization through lactide formation starts with a continuous condensation reaction of aqueous lactic acid to produce low molecular weight pre-polymer. After converted into a mixture of lactide stereo-isomers using tin catalysis the molten lactide mixture is purified by vacuum distillation. Finally, high molecular-weight polymer PLA is produced using a tin-catalyzed, ring-opening lactide polymerization in the melt. After the polymerization the remaining monomers are removed under vacuum and recycled to the beginning of the process. [5, 6, 22]

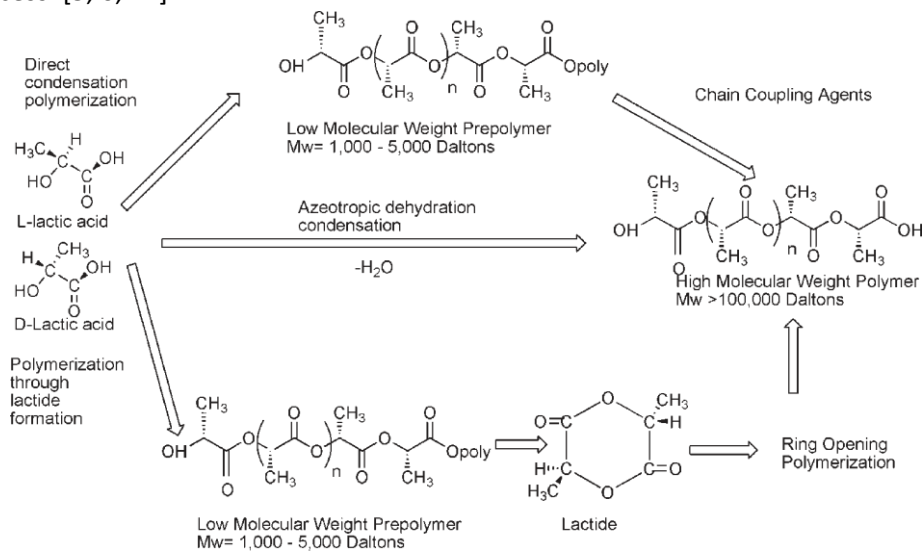


Figure 3: Different synthesis methods for obtaining high molecular weight PLA. [6]

Polymerization through lactide formation is the current method for obtaining polylactide polymers of high molecular weight, patented by Cargill Inc. in 1992, for commercial applications. The process combines the substantial environmental and economic benefits of synthesizing both lactide and PLA in the melt rather than in solution and, for the first time, provides a commercially viable biodegradable commodity polymer made from renewable resources. [5] The production of PLA presents numerous advantages: First of all, it can be obtained from a renewable agricultural source and its production consumes quantities of carbon dioxide. Thereby it provides significant energy savings and it is recyclable and compostable. It can help improve farm economies and the physical and mechanical properties can be manipulated through the polymer architecture. [6]

2.3.3 Applications

Based on the experimental research made until now it has been found that PLA is safe and generally recognized as safe (GRAS) for its use in food-contact articles. The research concludes PLA components migration by extraction tests in which samples of the polymer were exposed to food-simulating solvents. The conditions were reproduced in the most severe temperature/time to which food would be exposed while in contact with PLA. Results of this study [23] show that possible migration from the PLA polymer such as lactic acid, monomer lactide and linear dimer of lactic acid, lactoyllactic acid, are safe in food at levels far in excess of any small amount that might result from the intended use of PLA in food contact materials or articles. [1, 3] PLA has been widely studied for use in medical applications because of its bioresorbable and biocompatible properties and that it can be hydrolyzed in the human body such as in suturing material, surgical implants, drug-delivery systems and biologically active controlled release devices. [6, 18] The initial focus of PLA as a packaging material has been in high value films, rigid thermoforms, food and beverage containers and coated papers. Cargill Dow LLC started a company in 1997 to focus on the production and marketing of PLA with the intention of significantly reducing the cost of production and making PLA a large-volume plastic for a broader array of products. [5] This is a major landmark in the history of PLA because it's the start of a large-scale use of this biopolymer. [18] Nowadays, PLA has the potential for commercial large-scale production and applications in packaging due to its good transparency, and process ability with increased molecular weight. It is a stiff and rigid thermoplastic that can, depending on the stereochemistry of the polymer backbone, be totally amorphous or semi-crystalline. D-lactic acid monomers are incorporated to modify the crystallization behavior to have certain properties to make a wide variety of packaging materials. [3] At this time, PLA is being used as a food packaging polymer for short shelf life products such as containers, drinking cups, salad cups and lamination films for short shelf life products such as fruit and vegetables. Another current application is the use of PLA in compostable yard bags to encourage recycling and composting programs but new applications such as fibers, textiles, foamed articles and paper coatings are being pursued. [6]

2.3.4 Commercialization and Numbers

PLA is commercialized by different companies with different commercial names, like for example the Natureworks™ PLA produced by Natureworks LLC (Blair, NB).[1] But there are many other manufactures of PLA and lactide worldwide like Biomer, Birmingham Polymers, Inc., Boehringer Ingelheim, Galactic, Hycail, Mitsubishi Plastics, Inc., Purac and Shimadzu Corporation.[7] The global production of plastics in 2013 was estimated at some 299 million tons, representing a 3.9% increase over 2012's output. Today, the global plastic industry generates revenue of about \$600 billion annually. Packaging, representing 40% of demand in Europe and 42% in the United States, is responsible for the majority of plastic use. Nearly 10- 20 million tons of plastic, that breaks down into small fragments, end up in the oceans each year. Those fragments are consumed by sea life and transferred up the food chain, carrying chemical pollutants. [4]

2.3.5 Properties of PLA

The properties of high molecular weight PLA are determined by the stereochemistry of PLA and the molecular mass. The stereochemistry of PLA has a huge impact in the final polymer's thermal behavior, mechanical properties and thermo-mechanical performance. Therefore, the ability to control the stereo chemical architecture permits precise control over the speed of crystallization, the mechanical properties, the processing temperatures and the (bio)degradation behavior. Unlike petrochemical polymers, PLA will degrade primarily due to hydrolysis [6]; after several months of exposure to moisture, the chains begin to break down and degrade in two stages. The first is a reduction in molecular weight due to scission of the ester groups by non-enzymatic chain scission. Secondly, microorganisms can use low molecular weight PLA made from the bulk polymer producing carbon dioxide, water and humus. PLA can consist of three kinds of stereo isomers, namely L-lactide, D-lactide and meso-lactide while the molecular mass is controlled by the addition of hydroxylic compounds. [1, 3, 6, 22] For amorphous PLA, the glass transition temperature (T_g) is one of the most important parameters since dramatic changes in polymer chain mobility occur at and above T_g . For semi crystalline PLA, both the T_g and melting temperature (T_m) are important physical parameters for predicting PLA behavior. The melting point (T_m) for semi-crystalline PLA, depending on the structure, ranges from 130-230 °C and the T_g is about 62 °C. Above the T_g , PLA exhibits a major drawback of poor thermal resistance. T_g is determined by chain structure and increases with increasing molecular weight. [24]

Table 1: Physical properties of PLA. [1]

Experimental Data	PLA
T_g (°C)	62.1 ± 0.7
T_m (°C)	150.2 ± 0.5
Percent crystallinity (X_c)	29.0 ± 0.5
Oxygen transmission rate (OTR) (cc/m ² day) ^a	56.33 ± 0.12
Oxygen permeability coefficient (OPC) (kg · m · m ⁻² · s ⁻¹ · Pa ⁻¹) ^b	$1.21^{-18} \pm 0.07^{-18}$
Water vapor transmission rate (WVTR) (g · m ⁻² · day ⁻¹) ^a	15.30 ± 0.04
Water vapor permeability rate(WVPC) (kg · m · m ⁻² · s ⁻¹ · Pa ⁻¹) ^c	$1.89^{-14} \pm 0.08^{-14}$
^a Thickness of 20.0 ± 0.2 mils.	
^b OPC= OTR x l/ΔP, where l is the thickness in m and ΔP is the difference in oxygen partial pressure across the film.	
^c WVPC= WVTR x l/ΔP, where l is the thickness in m and ΔP is the difference in water vapor partial pressure across the film.	

As shown in Table 1, a 29% crystalline PLA polymer has a T_m of about 150,2 °C with a T_g of 62.1 °C. [3, 6] The density range for pure crystalline PLA is estimated at of 1.37-1.49 g/cc, in comparison with the 1.25g/cc for solid amorphous PLA. PLA has a lower T_g and T_m compared with PS and PET. The optimized crystallization temperature (T_c) is in the range of 105-115 °C. The density of amorphous poly (L-lactic acid) has been reported as 1.248 g/ml and for crystalline PLA as 1.290 g/ml. The surface energy of PLA is estimated at 45 dyn/cm and compared with other polymers like PE, PP, PET and PS only PET (49 dyn/cm) has a higher surface energy than PLA. "In general, the ability of a substrate to anchor inks, coatings or adhesives is directly related to its surface energy." [6] Considering the rheological properties of PLA, the shear viscosity affects thermal processing such as injection molding, extrusion, film blowing and thermoforming. The melt behavior of PLA is similar to polystyrene and the amount of plasticizer has a huge impact on the melt viscosity. In general, semi crystalline PLA has a higher shear viscosity than amorphous PLA. The melt flow index ranges from 8.51 g/10 min to 7.83 g/10 min at 200 °C and 5 kg of weight according to poly (98% L-lactide) and poly (94% -L lactide). PLA possesses intermediate water vapor barrier properties and has relatively intermediate oxygen barrier properties. The $O_2:CO_2$ permeability ratio of PLA is in the range of 1:7 to 1:12 and is therefore suitable for food packaging where high respiration is needed. [3, 6] PLA can be processed by sheet extrusion, injection and blow molding, thermoforming and film forming. PLLA polymers have a narrow processing window and can be plasticized with lactides, oligomeric lactic acid and a wide variety of conventional plasticizers to improve the brittle behavior of PLA. The tensile strength of PLA is lower than PET and within the range of PS. The absorption of visible and UV light by polymers can have a huge impact on the food quality due to their ability to affect flavor and the nutritional content such as in juices, vitamin and sport drinks, etc. Primary wavelengths between 200 and 2200nm gain interest in packaging application and can be divided into three components: Ultraviolet (UV) band (100-400nm) that can cause chemical reactions, visible spectrum (400-700nm) and near infrared band (700-2200nm). The UV band is divided in 3 parts, UV-A, UV-B and UV-C. UV-A is responsible for tanning and pigmentation of the human skin, UV-B causes the most photochemical degradation of plastics and UV-C generated by the sun never reaches the earth's surface. Studies have shown that nearly all the UV-B and UV-A light pass through a PLA film. Therefore, the application of transparent PLA films may require the use of additives to block UV light transmission to for the retention of taste and appearance, extension of shelf life and improvement of product quality of dairy products. Compared to other polymers, PLA transmits less UV-C light than LDPE but PET, PS transmit less UV-B and UV-C, which are the most damaging for food, than PLA and LDPE and PET does not transmit UV-C and UV-B wavelengths. In case of the visible light band, the yellow color of PLA bottles and trays can create a consumer's perception that the package is old due to the higher yellowness index of PLA while comparing to other polymers like PS, LDPE and PET.[6]Studies have shown that in the range of 25-45 °C poly (98% L-lactide) film has a higher CO_2 permeability coefficient than poly (94% L-lactide) and are both lower than the value for PS at 25 °C and 0%RH ($1.55 \cdot 10^{-16} \text{ kg} \cdot \text{m}/\text{m}^2 \cdot \text{s} \cdot \text{Pa}$) but higher than for PET (1.73 and $3.17 \cdot 10^{-18} \text{ kg} \cdot \text{m}/\text{m}^2 \cdot \text{s} \cdot \text{Pa}$ at 0%). The oxygen permeation coefficient (OPC) for PLA is $3.3 \cdot 10^{-17} \text{ kg} \cdot \text{m}/\text{m}^2 \cdot \text{s} \cdot \text{Pa}$ and an activation energy of 11.1 kJmol^{-1} . The OPC of PLA increase in the absence of moisture, showing figure 4.

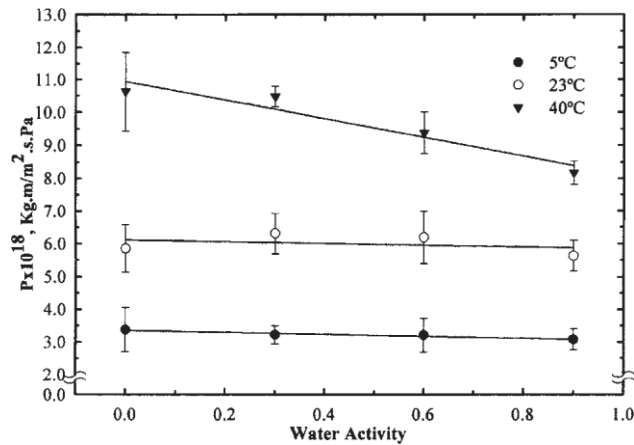


Figure 4: Oxygen permeability coefficient as a function of water activity for poly (98% L-Lactide). [6]

Poly (98% L-lactide) generates a more tortuous path for the permeation of oxygen molecules due to their higher crystallinity than poly (94% L-lactide). Compared to other polymers PLA is like PET hydrophobic and absorb very low amounts of water and show similar barrier property behavior. [6]

2.3.6 Crystallinity

Crystallinity is an important factor impacting the properties of PLA. The crystallization rate of PLA is relatively low compared with other semi-crystalline polymers. [24] Polymer morphology of PLA depends on the proportion of D and L-lactides providing a totally amorphous or up to 40 % crystallinity structure. The maximum achievable crystallinity is determined by the molecular weight and D-lactate content. PLA containing more than 93% L-lactic acid are semi crystalline while amorphous PLA contains 50-93% L-lactic acid due to the sufficient irregularity's from the presence of both meso- and D-lactide forms. [25] PLA can crystallize in different forms that refer to the space group patterns between the chains upon crystallization and depends on the preparation conditions of PLA. PLA usually crystallizes in the stable, orthorhombic α -form; however, β -form and γ -form are known to exist, as well as the recent discovery of the α' -form. The α' -form has a looser and less ordered chain packing than the α -form, leading into a lower modulus and barrier properties. Changes such as temperature and flow during processing can greatly influence the crystalline structure of PLA. Research has shown that the α' -form is only formed between 100 and 120 °C. [25] Even after any practical processing, PLA exhibits very low crystallinity. Amorphous PLA exhibits poor gas barrier properties and a short service life, which limits its use in fields such as hot fill packaging and durable applications. Therefore, PLA with a high crystallinity percentage is desired not only for its biodegradable, renewable and food-safe properties, but for improved mechanical and permeation performance as well. Drieskens *et al.* [26] reported that the crystallization of PLA causes a decrease of the oxygen permeability. The low crystallization rate is desirable for biaxial oriented films or stretch-formed bottles, while low Tg at this rate limits its use for other applications. [25, 27] Recent experimental results revealed the addition of oxalamide derivatives as a nucleating agent are soluble in PLA melt and capable of self-organizing into fibrils upon cooling. The crystallization rate and crystallinity of the PLA was significantly increased by the incorporation of 0.25–1.0 wt% of the tailor-made oxalamide derivatives. [28] This is one of the many ways to moderate the crystallinity of PLA, depending on the desired properties. One of the measurements investigated in this research is the crystallization rate of different PLA-MOF ratios.

2.3.7 Comparison of Mechanical Properties of PLA to Other Polymers

The respective values of mechanical properties of PLA in comparison with polypropylene (PP), polystyrene (PS), high density polyethylene (HDPE), polyamide (PA6) are shown in figure 5.

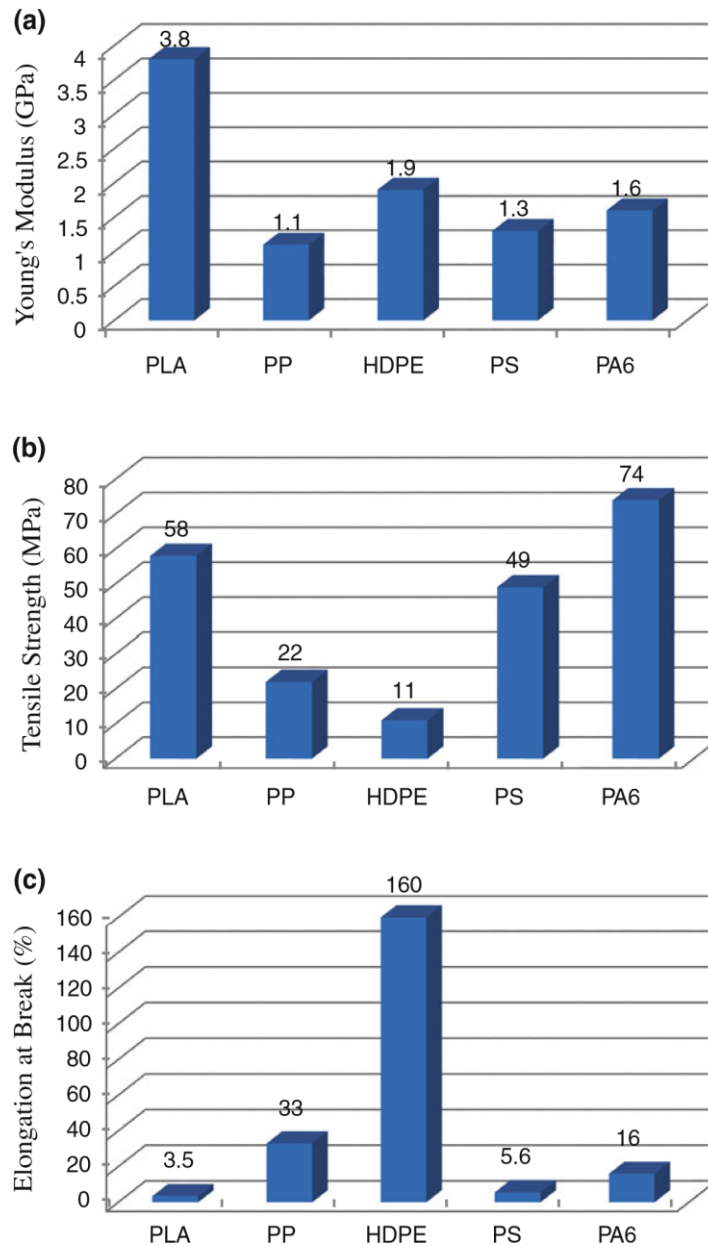


Figure 5: Mechanical properties of PLA and other commodity plastics. (a) Young's modulus, (b) Tensile strength and (c) Elongation at break. [29]

The elongation at break of PLA is lower than PS, proving that it is more brittle than PS resulting in a restricted use in a wide-range of applications. [29] PLA packages perform, as well as other containers made on synthetic polymer like PET, PS, etc., at room and low temperature and make them a good alternative for the same food application. PLA films and packages provide better mechanical properties than PS and have properties comparable to PET. However, some properties such as flexural properties, gas permeability, impact strength, process ability, low heat distortion temperature, high gas permeability, low melt viscosity etc., restrict their use in a wide-range of applications. PLA shows good barrier properties to aroma but the most important limitation on the use of PLA for food application packaging is the medium barrier to gases and vapors and the brittleness properties. [3] Therefore

modification of the biodegradable polymer through innovative technology has already proven to be an effective way to improve these properties concurrently.

2.3.8 PLA Blends

A possible strategy to decrease the brittleness and to enhance the properties of PLA is to make a blend between PLA and other polymers. Much research has been done in this area such as blending PLA with polymers obtained from glycerol acid, starch and PCL. Different mechanical and physical properties can be maintained depending on the application. There are generally 2 classes of polymer blends containing PLA; blends with other degradable/renewable resource polymers and blends with non-degradable polymer. Most widely studies polymer blends of PLA are those with PCL due to its low T_g and its rubbery characteristics which makes it an ideal candidate for toughening PLA. Other research containing PLA blends can be found elsewhere. [29]

2.4 PLA Bio Composites

To increase the mechanical performance or other important characteristics of PLA; PLA bio composites are a promising alternative. These bio composites are materials formed by a biodegradable PLA matrix (resin) and a reinforcing phase, for example fillers such as zirconia, magnesium oxide, hydroxyapatite. Three different groups of bio composite materials can be separated, 1) particulate composites, 2) fibrous composites, and 3) porous composites. [3]

2.4.1 PLA/Natural filler Composites

Natural fillers have a large variation in quality parameters such as strength, fineness, color and trash content and are receiving a lot of attention due to their stiffness enhancement, reduce cost along with maintaining the degradability of PLA. Natural fillers like kenaf, flax, jute and rice husk are already studied for the use in PLA composites to apply in the automotive, building materials and other industries.

2.4.2 PLA/Mineral Filler Composites

To improve the properties of PLA like rigidity, durability and hardness of PLA and to reduce the costs the use of mineral fillers such as mica, kaolin, calcium carbonate is already investigated. Talc for example has already proven to improve the stiffness, strength, and thermal resistance in PLA blends, although more studies are necessary to realize how the mineral fillers interact in the blend. For example, Carbon black (CB) was investigated on its mechanical and thermal properties of plasticized PLA. Although the improvement in stiffness was associated with the interaction between the PLA matrix and CB, this interaction caused an increase T_g of plasticized PLA. [29]

2.5 Nanocomposites

The term “nanocomposites” relates to the dispersion of nano-sized particles within the polymer matrix and gaining acceptance in the mainstream of the global plastics processing industry. They have an enormous potential in relation to a wide range of product development. The effect of the nanocomposites is currently under study but it is clear that these compounds could be a valid route to decrease the inherent rigidity of some biopolymers and to enhance their applications. Some of the nano-particles include layered silicates, hydroxyapatite, aluminum hydroxide and carbon nanotube.[3] Layered clay such as montmorillonite (MMT) is commonly used as a reinforcement material due to its nanoscale size and intercalation/exfoliation properties. The problem with these nanocomposites is mostly to disperse these composites in PLA. The most common strategy to overcome these difficulty is to replace the interlayer MMT cations with quaternized ammonium cations. Montmorillonite (MMT)-PLA composite has a 50% increase in the oxygen barrier properties and a 20% increase in the storage modulus when compared to neat PLA. [3] Nanocomposites in PLA results in very promising materials with improved properties with preservation of PLA’s biodegradability, without eco-toxicity and brings up some large improvements to the polymer matrix in terms of mechanical, fire retardant, rheological, gas barrier and optical properties, especially at low content (as small as 5 wt%) in comparison with conventional composites (>30 wt% of microfiller). Research concerning nanocomposites such as PLA with carbon nanotubes (CNT), cellulose nanowhiskers (CNW) can be found elsewhere. [29] It is shown that during crystallization interchain interactions precede intrachain interactions in the case of both intercalated nanocomposites and the neat polymer while the opposite behavior is seen in exfoliated nanocomposites. This may describe nonnucleating behavior of the organoclay previously seen in fully exfoliated nanocomposites. [30] In general, PLA nanocomposites represent a strong and emerging answer for improved and eco-friendly materials but still a lot of research has to be done concerning use of nanocomposites.

2.6 Porous Colloidal Articles

Porous colloidal particles have recently gained attention due to their large internal surface area and adsorbent potential. They are used in a widespread application in diverse fields, including sensing, catalysis, drug delivery and separations. [31] In the area of molecular inorganic-organic hybrid compounds, coordination compounds with infinite structures have been intensively studied. In particular, compounds with backbones constructed from metal ions as connectors and ligands as linkers, the so-called coordination polymers. Until mid-1990’s there were two types of porous materials, namely inorganic materials like the aluminosilicates and aluminophosphates, and carbon-based material. The activated carbons have a high open porosity and a high specific surface area, but have a disordered structure and will therefore not be discussed. [3, 32]

2.6.1 Adsorption/Adsorbents

Adsorption can be defined as an accumulation of atoms and molecules on the surface of a material. It is a surface phenomenon and depends on factors such as partial vapor pressure of the adsorbate, interaction between adsorbate and adsorbent, temperature, etc. The material’s surface atoms are not fully covered by their neighboring atoms, which helps to attract other atoms or molecules which results in a decreased surface energy. [3, 8] Adsorption is an exothermic process and performance characteristics of porous materials are determined by adsorption isotherms. These isotherms can be generated by the use of gravimetric, constant volume and dynamic adsorption methods.

Various adsorption models can be used to determine the adsorption such as the Langmuir and Brunauer-Emmett-Teller (BET) model. [8] There are 2 classes of the adsorption process depending on the nature of the bonding between the adsorbate molecule and adsorbant, namely (1) chemical adsorption (chemisorption) and (2) physical adsorption (physisorption). Chemisorption take place due to ionic, covalent or metallic bonds/coordinates and occurs or occurs to be not reversible. Physisorption is reversible and involves van der Waals interactions. [3, 8] An essential role to determinate of the properties of porous compounds involves the adsorption of guest molecules onto the solid surface and is governed by the interaction between guest molecules and the surface, pore size and shape. [32] The industrial adsorbents are categorized into three categories: 1) Oxygen based compounds that are polar and hydrophilic, e.g. zeolites and silica gel, (2) Carbon based compounds that are non-polar and hydrophobic, e.g. activated carbon and graphite, 3) polymer-based compounds that have polar or a-polar functional groups in the polymer. [3]

2.6.2 Zeolites

Zeolites belong to the family of microporous solids known as “molecular sieves” and are 3D crystalline, hydrated alkaline or alkaline-earth aluminosilicates and their framework is built from corner-sharing TO_4 tetrahedra (T=Al, Si). The framework forms a network of channels and cavities. The porosity is delivered through elimination of the water molecules. [3, 31] Extensive research has been done in natural and synthetic zeolites due to their intrinsic chemical reactivity, adsorptivity and ion exchange capacity. Sodium ions resent in zeolites can be substituted by silver ions to create good microbial properties. Ore other various transition metal ions are used to improve the electrical conductivity properties of the polymer composites. [3, 33] Many research has already been done concerning the effect of zeolites ($NaAlO_2$, SiO_2) and their dispersion in biopolymer PLA, with a particular interest in the improvement of antibacterial properties, permeability to water vapor, oxygen permeability and mechanical properties. [34] The aim of the study was to develop biodegradable plastics for active packaging of fresh produce by designing new composite materials based on PLA with zeolites to increase the shelf life of fresh products. Results show that, only with the use of a stabilizer (polyethylene glycol (PEG) with Mw: 1000 g/mol), the water vapor permeability and the oxygen transmission rate decreased upon the addition of zeolites while their mechanical properties improved. Also the bacteriostatic tests showed that these composites have very efficient anti-bacterial properties. [34] Other research [33] shows good interfacial adhesion between zeolite particles and PLA matrix using extrusion/injection compounding technique and an increased percent crystallinity of the PLA with the proportion of zeolites type 4A.

2.6.3 Other Common Adsorbent Materials

Other frequently used adsorbent materials include activated carbon, activated alumina and silica gel. Activated carbon is a form of carbon that is processed to obtain large volumes and a high surface area while activated alumina is widely used as a desiccant due to its large capacity to store water. Silica gel has a high moisture adsorption capacity and a large surface area resulting in the use of dehumidification processing. Adsorbents can be used to modify polymer properties in order to increase the adsorbent capacity of water or other compounds such as gases, vapor, liquids for use as functional membranes in different sorts of applications. [3]

2.7 Metal Organic Framework

2.7.1 Introduction

Metal Organic Frameworks (MOFs) is a class of crystalline compounds composed of metal ions linked together by organic bridging ligands forming one-, two-; or three-dimensional porous structures. [3, 8, 35] These sophisticated nanostructured materials have high porosity, ultrahigh surface areas, large pore sizes, affinity for certain molecules and micro-pore volume making them a promising candidate for high capacity adsorption of various gases and molecules. [8] Different MOF properties and structures can be achieved based on the selected metal and linker. For example, the geometry of the pores and the number of ligands that are bound to the metal and the orientation depends on the coordination preference of different metals. [3] Sadakiyo *et al.* [13] confirmed that the framework flexibility around the central metals of MOFs is related to the selective adsorption behavior. By selecting the appropriate building blocks and/or by post-synthetic modification their chemical environment can be adjusted. Gas separation in MOFs is based on 2 parameters, namely 1) the size-exclusion concerning variances in MOF pore holes and the kinetic diameter of gas particles, much like the action of a sieve, and 2) the different interaction powers between guests and the MOF framework. [36, 37] Many MOFs undergo structural changes upon adsorption of different molecules, also called breathing. [9] Guest particles can diffuse into the MOFs structure while the shape, affinity and size of these pores offer selectivity to the different types of gases. [38] Their open internal structures and long-range crystallinity and distinctive pore sizes can accommodate different types of gases such as CO₂, O₂, N₂, CH₄ and volatile organic compounds (VOCs). [3] This could be useful in packaging applications to selectively purge molecules that are considered unwanted in package because they can affect the quality of the product or the perception of the customer. [8] Their surface area is close to one order of magnitude higher than that of activated carbon and zeolites, namely between 1000 and 3000 m²/g or more. Table 1 compares the surface area of different industrial MOFs and other adsorbents. [3]

Table 2: Surface area of Basolite MOFs and other common used adsorbents. [3]

Materials	Langmuir surface area (m ² g ⁻¹)
Basolite A100 (Al-MOF)- Al-terephthalate	1100-1500
Basolite C300 (Cu-BTC-MOF) - Cu-benzene-1,3,5-tricarboxylate	1500-2100
Basolite F300 (Fe-EMOF) - Fe-benzene-1,3,5-tricarboxylate	1300-1600
Basolite Z1200 (Zn-EZIF) - Zn-2-methylimidazole	1300-1800
Basolite M050 (Mg-MOF) - Mg-formate	400-600
Zeolite	300-800
Alumina	110-470
Activated Carbon	250-950
Silica gel	400-600

2.7.2 Application of Metal Organic Frameworks

Murray *et al.* [39] provided the current status of hydrogen storage within metal organic frameworks in the aim to use hydrogen as a clean alternative to hydrocarbon fuels. $Zn_4O(BDC)_3$ has successfully been used for cryogenic hydrogen storage at 77 K and pressures up to 100 bar with a reversible H_2 uptake of 10.0 total wt% and 66 g/L. [39] Other applications include gas purification, gas separation, storage media, drug delivery carriers and heterogeneous catalysis. [3, 36] Latest research concerns metal-organic frameworks effectively functionalized with amino groups to significantly enhance the affinity for CO_2 , resulting in a very large selectivity in CO_2/CH_4 separations. [40]

2.7.3 Al - MOF

Light weight metals such as alkali earths (magnesium, calcium) and aluminum as inorganic nodes are used as building blocks, with aluminum as the most promising candidate due to the interconnection of aluminum-centered octahedral that allows the formation of numerous one- or two-dimensional inorganic sub-networks. Next to the global key properties of MOF like high surface areas and minimal dead volume, Al-MOF surpass in stability towards water which prolongs their lifetime, rendering their wide-ranging use economically more worthwhile. Al-MOF are therefore used for methane storage in the aim to require natural gas for alternative energy resources or for the purification of air and water as well as heating/cooling applications. [16]

2.7.4 Mil-53 Series

MIL-53 series is a special class of MOF materials with 1-D diamond shaped pores with a free diameter of 8.6 Å build from $MO_4(OH)_2$ octahedra (M referring to Fe^{3+} , Cr^{3+} , Al^{3+} , Ga^{3+} , In^{3+} or Sc^{3+}) and 1,4-benzenedicarboxylate (terephthalate) linkers. MIL-53 Aluminum exhibits extraordinary thermal stability up to 450 °C and its members reversibly uptake/release water and its high hydrothermal stability is due to the strong Al-O bonds and octahedral coordination of aluminum. [16] Many researchers focused their attention on it due to its high thermal and chemical stability and the ability to reversibly change their framework when guest molecules are introduced. [15] This phenomenon, also called the breathing effect allows the pores to reversibly contract or open upon adsorption of molecules. [9] Loiseau *et al.* [41] reported that water hydrogen bonding being responsible for the switching between the MIL-53 ht (high temperature) and MIL-53 lt (low temperature) forms. Lifang *et al.* [35] investigated the effect of adding MIL-53 (Al) on the performance of PMIA membranes and the potential application in organic nanofiltration.

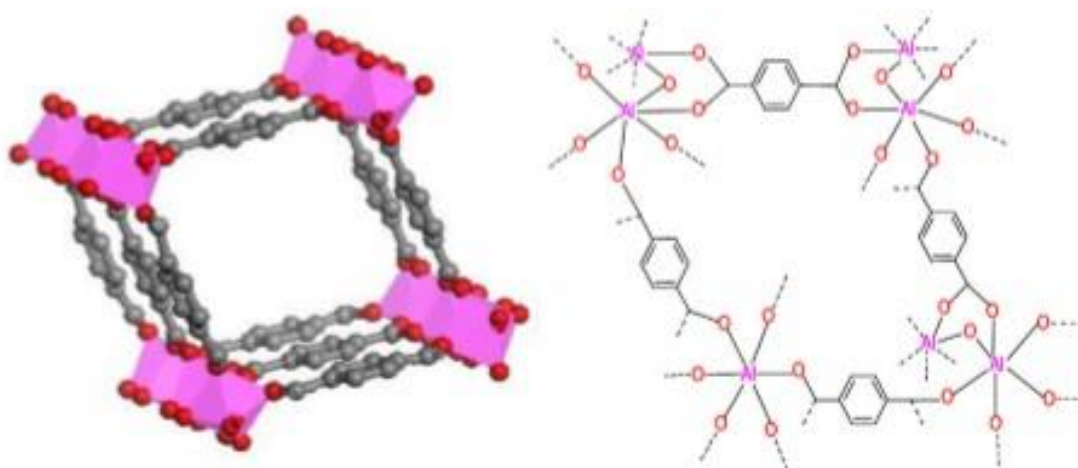


Figure 6: Structure of MIL-53 adapted from Yan *et al.* [42]

2.7.5 Synthesis

Aluminum 1,4-benzenedicarboxylate $\text{Al}(\text{OH})[\text{O}_2\text{C}-\text{C}_6\text{H}_4-\text{CO}_2]$. $[\text{HO}_2\text{C}-\text{C}_6\text{H}_4-\text{CO}_2\text{H}]_{0.70}$ or MIL-53 as (Al) can be synthesized by heating a mixture of aluminum nitrate, 1,4-benzenedicarboxylic acid and water at 220 °C. The created 3D framework exists of infinite trans chains of corner-sharing $\text{AlO}_4(\text{OH})_2$ octahedra. The 1,4-benzenedicarboxylate (BCD) groups interconnect the chains resulting in 1D rhombic-shaped tunnels. After evacuate the disordered 1,4-benzenedicarboxylic acid molecules that were trapped inside these tunnels by heating the mixture between 275 and 420 °C, the nanoporous open-framework with empty pores is achieved. [41]

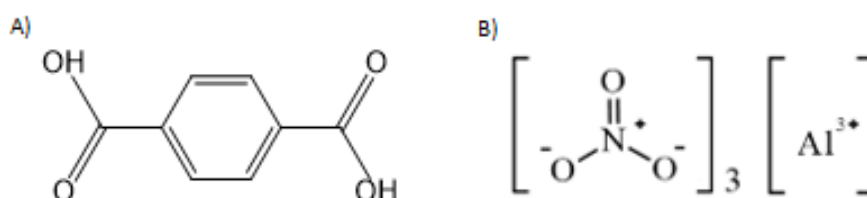


Figure 7: Structure of A) 1,4-benzenedicarboxylic acid and B) Aluminum nitrate.

2.8 Mixed Matrix Membranes (MMMs)

2.8.1 Introduction

To improve the functionality of polymer based membranes, researchers have developed new mixed matrix membranes (MMM) where a homogeneous dispersion of filler particles in a polymeric matrix is established. [8, 9] MMMs combines the advantage of the high permeability and selectivity of the fillers with the simplicity of preparing polymer-based membranes. [36] It's morphology and separation performance depends both on the polymer and filler properties. The presence of various mesoporous or microporous fillers such as zeolites, carbon molecular sieves have already proven to show an increased permeability effect and enhance the separation properties of MMM. Unfortunately, matrix sub-micron size holes can come into existence due to the poor compatibility between the inorganic fillers and organic polymeric making these MMM not as effective as expected for gas separation applications. [10, 11] The newest interest goes therefore to MOF particles due to their strong interfacial interactions between MOF and the polymer and their good thermal stability. [12]

2.8.2 MMMs Including MOF

Yehia *et al.* [43] first explored with incorporating MOFs into a polymer matrix for gas separation by using copper (II) biphenyl dicarboxylate-triethylenediamine poly(3-acetoxyethylthiophene) mixed matrix membranes for methane facilitated transport. Gas separation membranes based on polyimides with metal-organic framework (MIL-101) compounds have been surveyed by Klyamkin *et al.* [44] ; this resulted in increased permeability for a number of gases by 3-5 orders of magnitude. Thanks to the vast possibilities of MOF in terms of design and their intrinsic hybrid nature, this field of research has experienced a rapid growth. [9]

2.9 PLA - MOF Mixed Matrix Membranes

Mixed matrix membranes containing a PLA matrix and MOF filler have already been studied. For instance, a new class of PLA fibers containing cobalt-based MOF were reviewed using SEM analysis by Quiros *et al.* [45] The results showed that these fibers were less susceptible to bacterial colonization and biofilm formation. These results were confirmed by confocal microscopy and quantitative tests for microbial growth assuming that PLA-MOFs provide antibacterial activity suitable for various biomedical applications. [45] Many researchers have investigated the use of MOF particles in PLA by fabricating mixed matrix membranes to increase the permeability of various gases, water molecules and organic compounds in PLA membranes for industrial applications such as gas separation and packaging. Kathuria A. *et al.* [12] studied the effect of $\text{Cu}_3(\text{BTC})_2$ MOF in PLLA matrix on different gases (CO_2 , O_2), H_2O and organic aroma compounds (trans-2-hexenal, acetaldehyde) by mass transfer and permselectivity. Results show that an addition of 20% (w/w) $\text{Cu}_3(\text{BTC})_2$ MOF increased the carbon dioxide and trans-2-hexenal permeability due to strong physisorption type interaction between the gas molecules and the MOF unlike the aromatic or water molecules who did not show any changes in the mass transfer properties. [12] Next to enhancing the permeability properties of PLA by the Activated $\text{Cu}_3(\text{BTC})_2$ MOF, studies [14] show that PLLA - $\text{Cu}_3(\text{BTC})_2$ MOF composites improved the toughness of the composites compared to neat PLLA. SEM and rheological studies indicated that the cavitation induced by debonding at the interface of PLLA and $\text{Cu}_3(\text{BTC})_2$ MOF particles caused these improving toughness of the composites during uniaxial stress.

2.10 Solvent Casting

The solvent casting technique is frequently used to prepare biopolymer films and involves solubilization, casting, and drying. PLA is highly soluble in solvents such as methylene chloride, chloroform, dioxane and benzene. Film properties are influenced by the use of each solvent, for instance the use of dioxanes causes a rough film surface due to its slow evaporation rate. Chloroform induces a greater chain mobility of the polymer which will enhance the interaction with the MOF particles. Byun *et al.* [46] reported the effect of different solvent mixtures on the properties of solvent casted PLA films, resulting that the solvent choice has an impact in crystallization and thermal expansion stability. The use of methylene oxide showed the highest crystallization rate and thermal expansion stability, but affected the mechanical ability due to its brittleness. [46]

3 Synthesis of PLLA - MOF MMMs

3.1 Introduction

In this chapter the synthesis of the PLLA-MOF composites is discussed. Starting with the methodology of the used materials followed by the sample preparation and compression molding.

3.2 Methodology

3.2.1 Materials

Poly (L-lactic acid) (PLLA) resin grade 4043 D, (98% L-lactide) pellets were supplied by NatureWorks LLC (Blair, NE, USA). The weight average molecular weight (M_w) was 111 kDa, with a number average molecular weight (M_n) of 84 kDa and a polydispersity index (M_w/M_n) of 1.3. Metallic organic framework, MOF, compounds were produced from Sigma-Aldrich (St. Louis, MO, USA) under the trade name of Basolite™ A100 MOF ($C_8H_5AlO_5$), with a surface area between 1,100 and 1,500 m^2g^{-1} and particle size distribution 31.55 μm . Chloroform [anhydrous $\geq 99\%$] was purchased from Sigma-Aldrich (St. Louis, MO, USA).

3.2.2 Sample Preparation

PLLA pellets were dried at 80 °C for 4 hours using a Thermo Scientific VWR Oven (Fisher Scientific, Pittsburg, PA, USA) with a negative pressure of 22 mmHg and packed in an air tight glass bottle. 3 grams of dried PLLA pellets were gradually poured into 75 ml of chloroform at 23 °C while mixing the solution with a magnetic stir plate (Thermo scientific, MO: SP136424) rotating at 300RPM for approximately 90 minutes until all PLA pellets were dissolved. Basolite™ A100 MOF ($C_8H_5AlO_5$) MOF particles were crushed by applying light, concentric pressure using a Green Marble Mortar & Pestle (Creative Home, Manalapan, NJ, USA). PLLA, PLLA - 1% MOF, PLLA - 5% MOF, PLLA - 10% MOF and PLLA - 20% MOF were processed by solvent casting. The desired MOF ratio was weighed out using a Mettler Toledo Scale, Model ME54E (Columbus, OH, USA) and poured in the dissolved PLLA-chloroform solution while mingling the solution with a magnetic stir plate (Thermo scientific, MO: SP136424) rotating at 300RPM for 10 seconds. Ultrasonication was performed on the PLLA-MOF-chloroform solution using a Q500 Ultrasonicator purchased from QSonica, LLC (Newtown, CT, USA). An on-off cycle was programmed to ultrasonicate for 3 minutes, with an on cycle time of 3 seconds and a frequency of 20,000 Hz, and the off cycle 0 Hz and 2 seconds alternating respectively. The ultrasonicated solution was poured into 3 molds of a Good Grips Mini Muffin Pan, purchased from Oxo (Chambersburg, PA, USA) and covered with two layers of tin foil, taped around the sides and placed in the fume hood. The evaporation rate of chloroform was controlled by poking a small hole in the thin foil, approximately 3mm in diameter, just above the center of each mold. After 4 days the solid samples were removed from the mold and transferred to a Thermo Scientific VWR Oven, at 23 °C with a negative pressure of 22 mmHg, until all the chloroform was evaporated out of the samples. Samples were stored in vacuum bags at room temperature until the beginning of the different tests. *Figure 8* shows the PLLA - MOF composites. It was observed that MOF particles gathered together resulting in a non-homogeneous dispersion. The MOF-particles also have the intention to sink to the bottom. An increase in MOF particles in the MMM resulted in more brittle and darker samples.

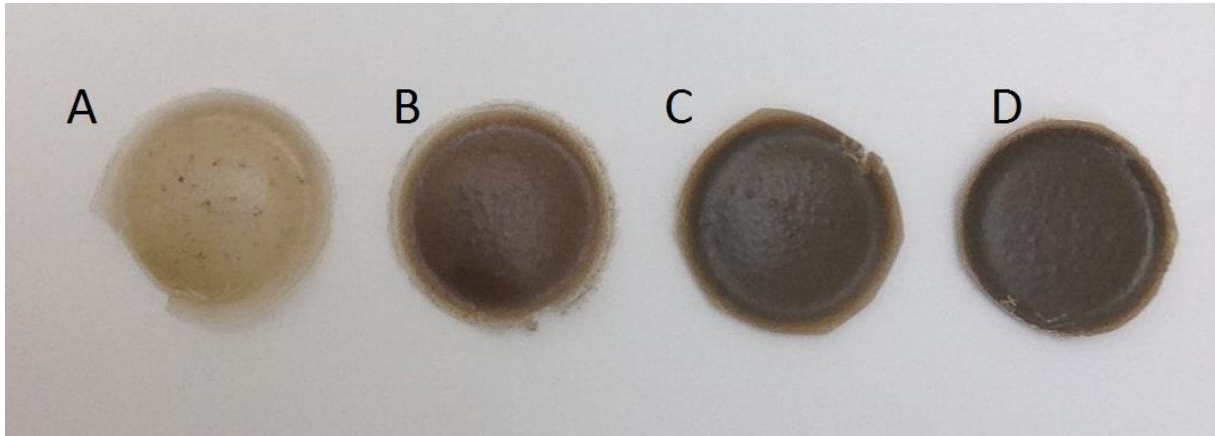


Figure 8: Solvent casted PLLA-MOF samples after a total of 20 days. A: PLLA - 1% MOF. B: PLA - 5% MOF. C: PLLA - 10% MOF and PLA - 20% MOF.

3.2.3 Compression Molding

Solvent casted samples were compression molded with a compression molder to reduce the thickness for permeability tests. The solvent casted samples were placed between thin Teflon sheets and positioned in the middle of the compression molder plates and heated up until 170 °C for 10 minutes, until the samples were melted. A force of 6000 lbs was applied on the samples for 5 minutes and cooled at room temperature afterwards.

4 Characterization of PLLA - MOF MMMs

FTIR analysis of the mixed matrix membranes were performed to study the bonds and chemical interactions in membranes. DSC was executed to determine the thermal properties and the crystallinity of the membranes. TGA studies were performed to investigate the thermal stability of the membranes. Membranes morphology and MOF particle dispersion in the polymer matrix were evaluated using SEM analysis.

4.1 Fourier Transform Infrared Spectroscopy

Fourier Transform Infrared Spectroscopy of Al - MOF, neat PLLA and PLLA - MOF MMMs was performed using a FTIR IRaffiny-1S (DE, USA). The spectra were captured in absorption mode at room temperature, in the range of 4000 - 400 cm^{-1} with a resolution of 2 cm^{-1} and 40 accumulated number of scans. The background spectra used for reduction were collected at the room temperature and samples were examined in triplet.

4.2 Differential Scanning Calorimetry

DSC analysis of neat PLLA and PLLA - MOF MMMs was investigated using a DSC Q1000 (TA instruments). Samples between 5 and 10 mg were perforated from the MMM and non-hermetically sealed in an aluminum pan and placed with the reference pan in the DSC cell and run in triplicates. Heat/cool/heat cycles from 0 °C to 180 °C at a rate of 10 °C min^{-1} were performed under a constant nitrogen flow. To disregard the thermal history during processing or storage, the second heating cycle was used to determine the glass transition (T_g) temperature, cold crystallization onset (T_{co}), melting temperature (T_m) and to calculate the enthalpy of cold crystallization (ΔH_c) and fusion (ΔH_m). The percent crystallinity X_c (%) was estimated using the following equation:

$$X_c(\%) = \frac{\Delta H_m - \Delta H_c}{\Delta H_m^c(1-x)} \times 100$$

With ΔH_m^c referring to the enthalpy of fusion of pure crystalline PLA; $\Delta H_m^c = 93,1 \text{ J/kg}$ and x represents the mass fraction of MOF in the MMM. [14] Universal Analysis software version 2000 (TA Instruments) was used to analyze the data and samples were run in triplicates.

4.3 Thermogravimetric Analysis

Thermogravimetric analysis of AL - MOF, neat PLLA and PLLA - MOF MMMS was investigated using a TGA Q50 (TA instruments, DE USA) under nitrogen flow of 20ml/min. Samples between 5 and 10 mg were perforated from the MMM and placed in an aluminum pan before heated at a rate of 10 °C/min from room temperature to 600 °C. Universal Analysis software version 2000 (TA Instruments) was used to analyze the data and samples were run in triplicates.

4.4 Scanning Electron Microscopy

Morphological analysis was performed using a SEM Philips Quanta 200 on Low Vacuum mode (100 Pascals) with the use of a tungsten filament. SEM micrographs of MOF, neat PLLA and PLLA - MOF MMM were obtained at an accelerating voltage of 12.5 kV.

5 Results and Discussion

In this section the results and discussions are presented for the different characterization studies of the PLLA - MOF MMMs.

5.1 Fourier Transform Infrared Spectroscopy

Figure 9 shows the FTIR spectrum of neat PLLA. The general band assignments and intensity for PLLA provided in the literature and experimental are presented in Table 3. [18, 47, 48] Results show that the majority of the experimental FTIR spectra corresponds with the literature. CH₃ and CH stretching regions were observed between 3000 and 2900 cm⁻¹. For the C=O stretching region a broad asymmetric band appeared at 1753 cm⁻¹ and CH₃ and CH deformation were responsible for the bands between 1450 - 1350 cm⁻¹. The appearance of the ester group was shown by the C-O stretching modes at 1180 cm⁻¹ and the C-O-C asymmetric mode at 1080 cm⁻¹. The band at 874 cm⁻¹ and 760 cm⁻¹ were assigned to the stretching mode of C-COO and C=O deformation, respectively.

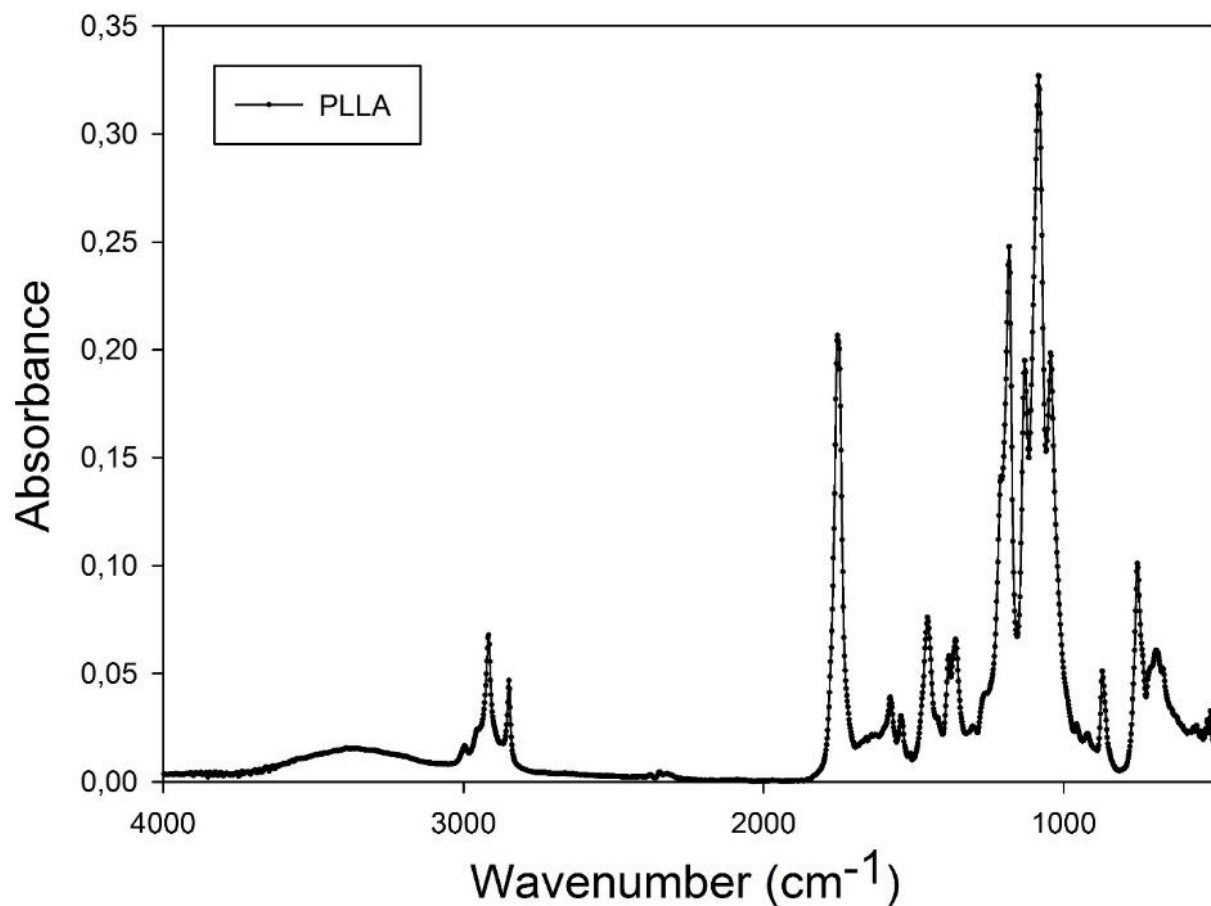


Figure 9: FTIR spectrum of neat PLLA.

Table 3: Wavenumbers (cm^{-1}) and vibrational assignments of neat PLLA.

Literature		Experimental	
IR (cm^{-1})	IR (cm^{-1})	Intensity	Assignments
2997	2977	medium	$\nu_{\text{as}} \text{CH}_3$
2947	2952	medium	$\nu_{\text{s}} \text{CH}_3$
2881	2918	Weak	νCH
1760	1753	very strong	$\nu \text{C=O}$
1452	1456	strong	$\delta_{\text{as}} \text{CH}_3$
1348-1388	1358	strong	$\delta_{\text{s}} \text{CH}_3$
1215-1185	1180	very strong	$\nu_{\text{as}} \text{COC} + r_{\text{as}} \text{CH}_3$
1130	1132	strong	$r_{\text{as}} \text{CH}_3$
1100 - 1090	1080	very strong -shoulder	$\nu_{\text{s}} \text{COC}$
1045	1043	strong	$\nu \text{C-CH}_3$
875-860	874	medium - shoulder	$\nu \text{C-COO}$
760-740	754	strong - shoulder	$\delta_{\text{s}} \text{C=O}$
711-677	685	medium	$\gamma \text{C=O}$

Figure 10 represents the FTIR spectrum of MIL - 53 (Al). The general band assignments and intensity for MIL-53 (Al) provided in the literature and experimental are presented in Table 4. [15, 41, 49] Results show that the majority of the experimental FTIR spectra corresponds with the literature.

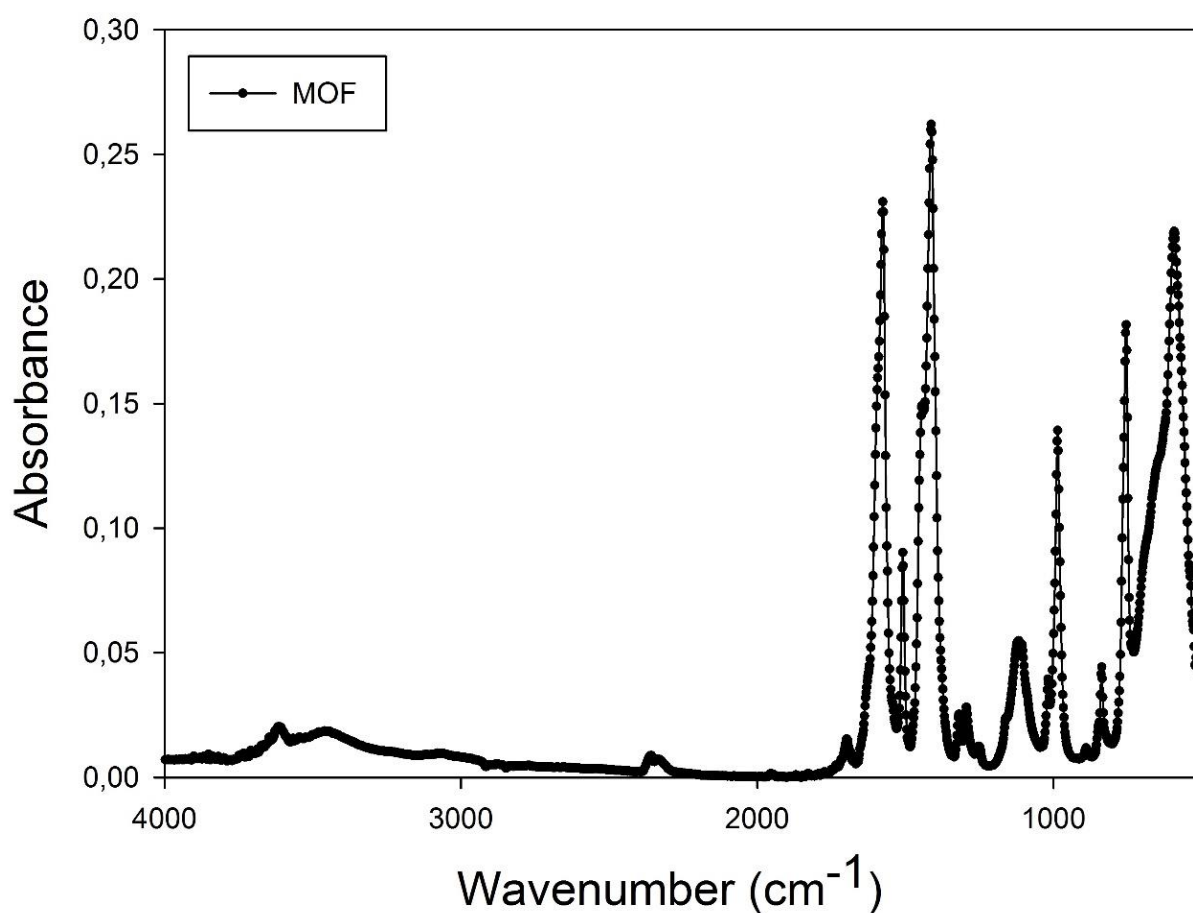


Figure 10: FTIR spectrum of MIL-53 (Al).

Table 4: Wavenumbers (cm^{-1}) and vibrational assignments of Mil-53 (Al).

Literature	Experimental		
IR (cm^{-1})	IR (cm^{-1})	Intensity	Assignments
3500-3000	3500-3000	Weak	$\nu_{\text{as}} \text{OH}$
1604-1503	1578	Strong	$\nu_{\text{as}} \text{CO}(\text{CO}_2)$
1435	1410	Strong	$\nu_{\text{s}} \text{CO}(\text{CO}_2)$
1150	1101	Medium	δCH
1070-1121	986	Strong	δOH
703	754	Strong	γCCC
600-500	590	strong	$\delta/\nu \text{AlOAl}$

Figure 11 represents the FTIR spectrum of neat PLLA, MOF and PLLA - MOF MMMs. An overall trend occurred showing a higher absorbance for PLA - 1%MOF followed by PLLA - 5% MOF, PLLA - 10% MOF, neat PLLA and PLLA - 20% MOF for the most prominent PLLA peaks. The presence of MOF was observed in the region of 3500 - 3000, 1420 - 1400 and 600 - 500 cm^{-1} assigned to hydroxyl groups bridging the aluminum in the inorganic component, $\nu_{\text{s}} \text{CO}(\text{CO}_2)$ and to $\delta/\nu \text{AlOAl}$, respectively. The peaks in the PLLA - MOF MMMs assigned to the MOF particles increased by adding more MOF to the PLLA matrix. No band shifts or new band peaks were observed by the addition of MOF showing that no chemical reactions occurred.

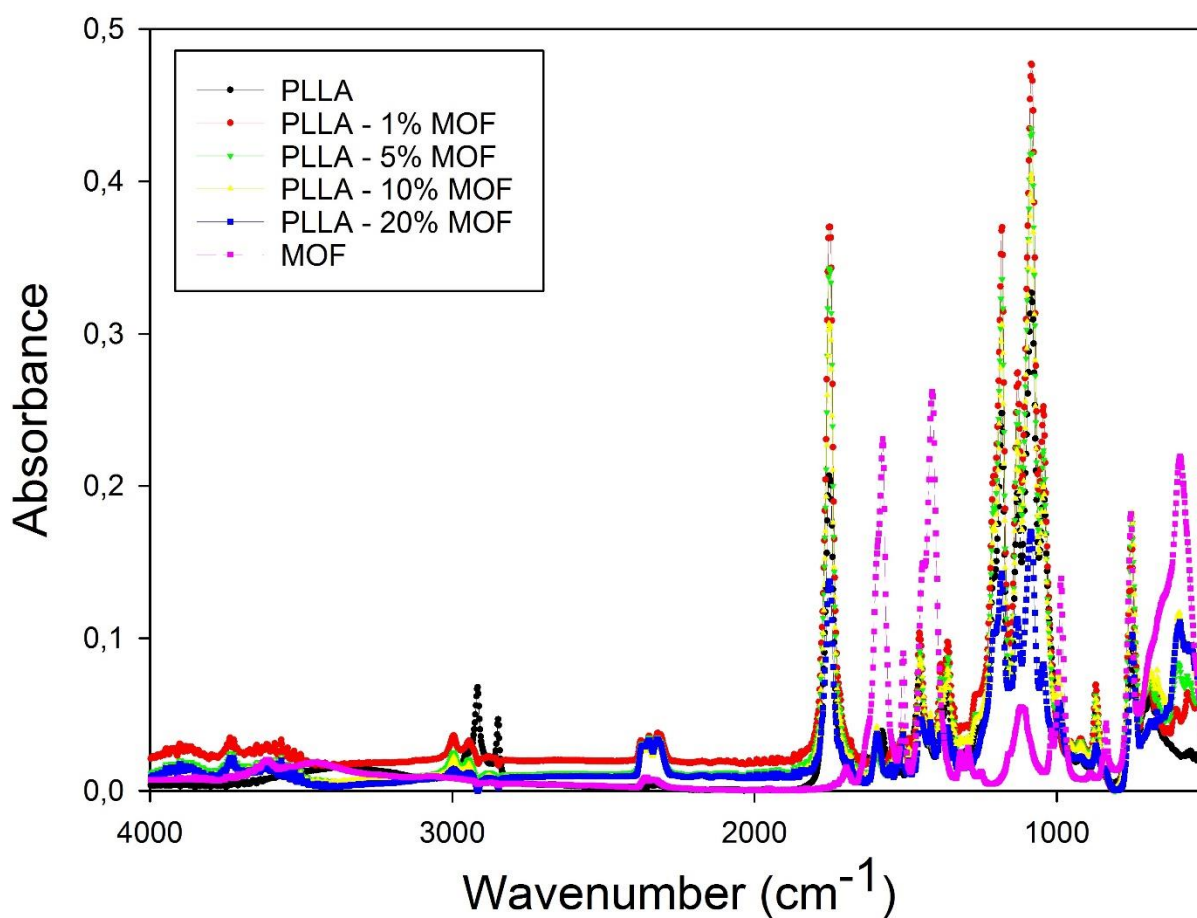


Figure 11: FTIR spectrum of neat PLLA, AL - MOF and PLLA - MOF MMMs.

Literature reported that the backbone stretching and CH₃ rocking region between 960 - 830 cm⁻¹ is sensitive to the degree of crystallization of PLLA (figure 12). [30, 50] The peak at 923 cm⁻¹ can be assigned to the coupling of C-C backbone stretching with the CH₃ rocking mode. An increase in this peak results in a more prominent presence of the 10₃ helix chain conformation of PLLA α crystals. [51]

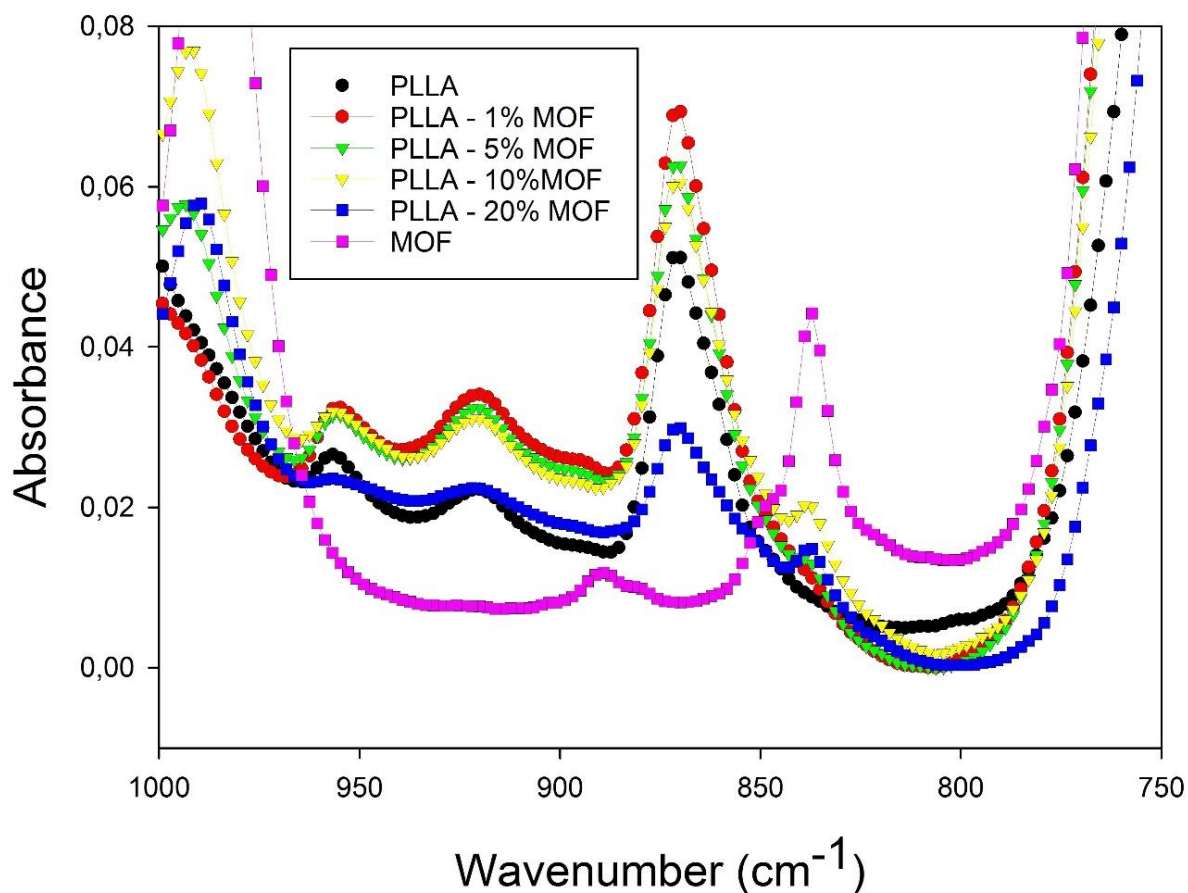


Figure 12: FTIR spectra of neat PLLA and PLLA - MOF MMMs for the 1000 - 750 cm⁻¹ region.

To investigate the change that occurred in this region due to the additional MOF content, the area under the peak was calculated and results are shown in *Table 5*. The addition of 1% MOF resulted in the largest area under the peak referring to the highest crystallinity and decreased by adding more MOF wt% to the PLLA matrix. The results revealed that the addition of MOF particles to the PLLA matrix resulted in a decrease in crystallinity.

Table 5: Area under peak 923 cm⁻¹ related to the crystallinity of PLLA calculated by FTIR results.

Samples	Area under peak 923 cm ⁻¹
PLLA	0.04675 ± 0.002503 ^A
PLLA + 1% MOF	0.07132 ± 0.004474 ^B
PLLA + 5% MOF	0.061463 ± 0.007891 ^{A,B,C}
PLLA + 10% MOF	0.058367 ± 0.000673 ^C
PLLA + 20% MOF	0.02468 ± 0.000877 ^D

Mean ± standard deviation followed by the same superscript in the same column are not statistically significantly different ($p > 0.05$).

5.2 Differential Scanning Calorimetry

DSC thermograms derived from the 2nd heating cycle are presented in Figure 13. The addition of MOF particles to the PLLA matrix resulted in an increase in glass transition temperature (T_g), a decrease in cold crystallization (ΔH_c) and fusion enthalpy (ΔH_m).

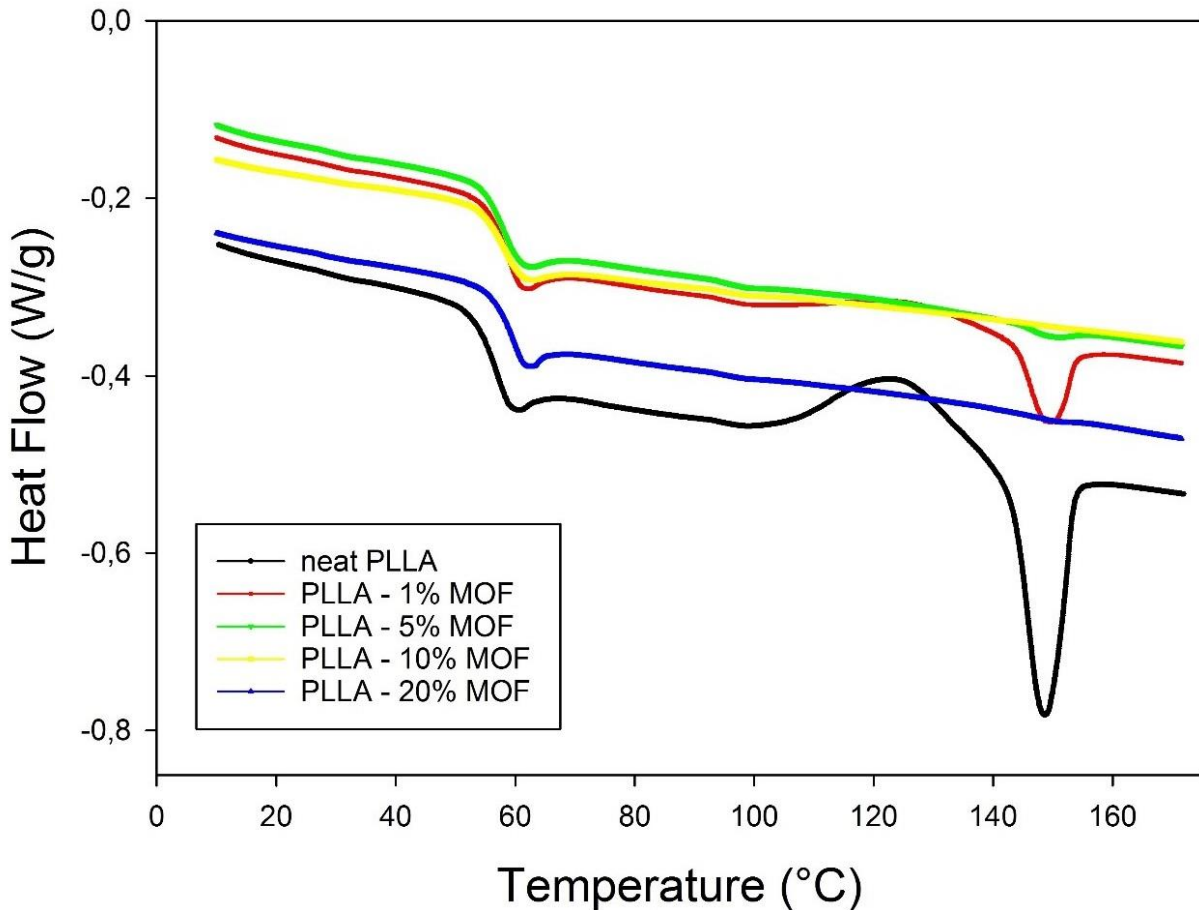


Figure 13: DSC thermograms of neat PLLA and PLLA - MOF MMMs derived from the 2nd heating cycle with a heating rate of 10 °C min⁻¹.

Table 6 shows the thermal characteristics of neat PLLA and PLLA - MOF MMMs derived for the 2nd heating cycle. Results showed that the enthalpy of cold crystallization decreased from around 8.68 J/Kg to 2.72 J/Kg for PLLA and PLLA - 1% MOF respectively. There was no T_{co} and ΔH_c observed in PLLA - 5% MOF, PLLA - 10% MOF and PLLA - 20% MOF suggesting that MOF particles hinder the PLLA chains to crystallize. Table 6 shows that PLLA has a 3.23 percent crystallinity, which suggests that solvent casted samples were nearly amorphous. The enthalpy of fusion (ΔH_m) for neat PLLA was estimated at 11.69 J/Kg and decreased to 4.69 J/Kg and 0.46 J/Kg for PLLA - 1% MOF and PLLA - 5% MOF respectively. There was no T_m and ΔH_m observed in PLLA - 10% MOF and PLLA - 20% MOF suggesting that these MMMS were already in their liquid state after undergoing the glass transition. Amorphous polymers soften gradually as the temperature rises and don't show a sharp melt point due to their randomly ordered molecular structure. [18]

Table 6: Thermal characteristics of neat PLLA and PLLA - MOF MMMs derived from the 2nd heating cycle.

Sample	Cold Crystallization			Melting		Crystallinity
	T _g (°C)	T _{co} (°C)	ΔH _c (J/Kg)	T _m (°C)	ΔH _m (J/Kg)	X _c (%)
PLLA	56.59 ± 0.49 ^A	105.10 ± 1.22 ^A	8.68 ± 1.93 ^A	148.35 ± 0.40 ^A	11.69 ± 2.17 ^A	3.23 ± 0.09 ^A
PLLA - 1% MOF	59.03 ± 0.52 ^B	108.59 ± 4.19 ^A	2.72+2.64 ^B	148.97 ± 0.19 ^{A, B}	4.69 ± 2.76 ^B	3.09 ± 0.04 ^A
PLLA - 5% MOF	57.90 ± 0.3 ^C	-	-	149.41 ± 0.39 ^B	0.46 ± 0.07 ^C	0.49 ± 0.08 ^B
PLLA - 10% MOF	57.27 ± 1.42 ^{A,B,C}	-	-	-	-	-
PLLA - 20% MOF	60.11 ± 0.62 ^B	-	-	-	-	-

Mean ± standard deviation followed by the same superscript in the same column are not statistically significantly different ($p > 0.05$). The '-' symbol denotes no results were obtained.

Figure 14 shows the percentage crystallinity of neat PLLA and PLLA - MOF MMMs. Crystallinity decreased by around 4% for PLLA - 1% MOF and 85% for PLLA - 5% MOF as compared to neat PLLA. PLLA - 10% MOF and PLLA - 20% MOF showed no crystallinity percentage resulting in completely amorphous MMMs. The decrease in crystallization could be associated with MOF particles hindering PLA chain mobility within the matrix.

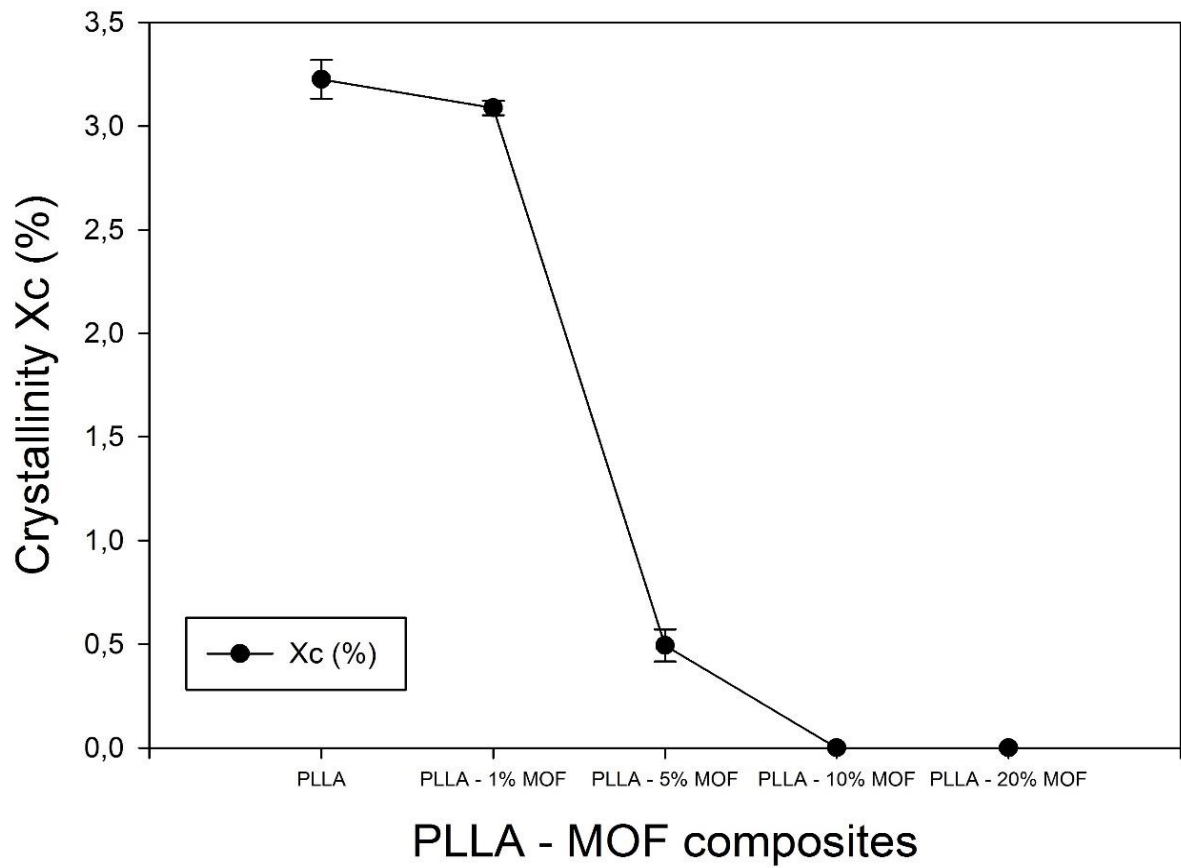


Figure 14: Crystallinity of neat PLLA and PLLA - MOF MMMs derived from 2nd heating cycle of DSC test.

5.3 Thermogravimetric Analysis

Figure 15 illustrates temperature-dependent weight loss curves for neat PLLA and PLLA - MOF MMMs in nitrogen for the temperature range of 50 - 600 °C. The complete thermal degradation occurred in 2 steps for neat PLLA and in 3 steps for the PLLA - MOF MMMs. The first significant weight loss occurred due to the evaporation of the volatile compounds between 100 and 200 °C. Degradation of the PLLA took place between 200 and 400 °C and represents the 2nd step. The last step characterized the degradation of the MOF particles starting from 550 °C. MOF particles showed thermal stability up to 500 °C. [41] The addition of MOF to the PLLA matrix resulted that the polymer thermally decomposed more easily, as can be seen by the TGA curves shifted towards lower temperatures. It can therefore be suggested that the MOF particles reacted as depolymerization catalyst for PLLA and increased the activation energy of degradation. [52, 53]

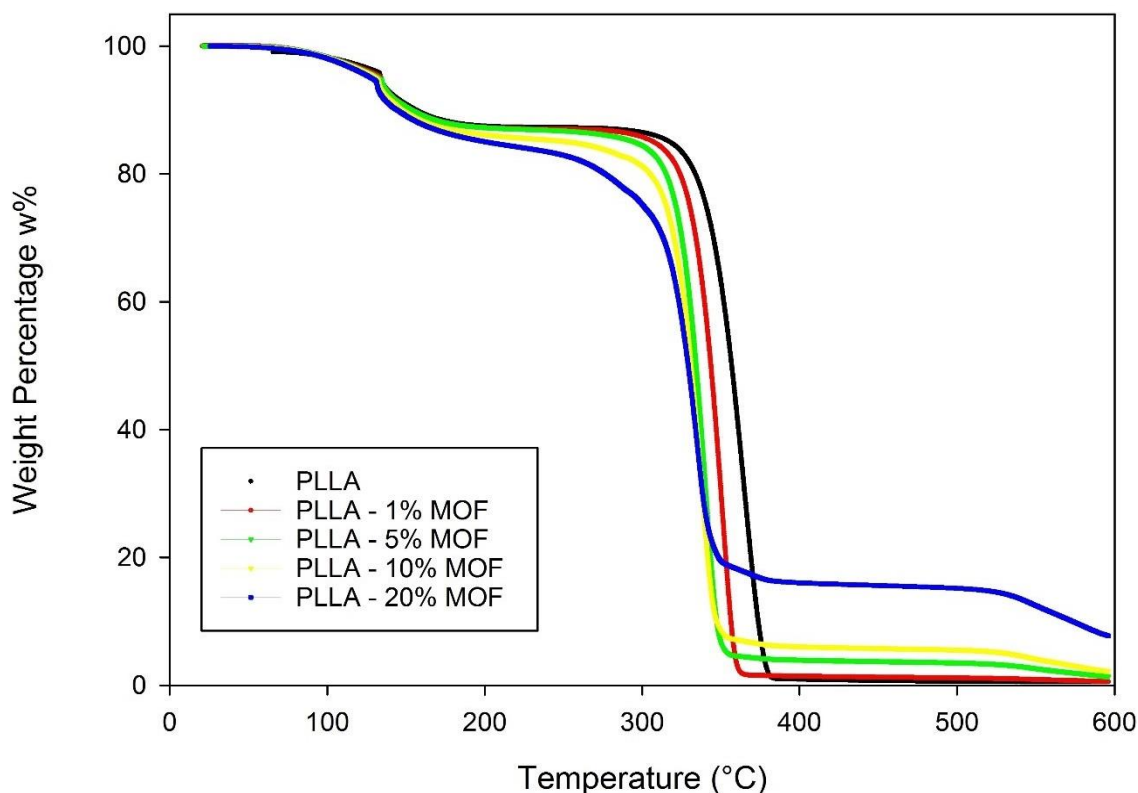


Figure 15: TGA curves for PLLA and PLLA - MOF MMMs in the range of 50-600 °C.

Table 7 summarizes the onset temperature of evaporation of volatile compounds (T_{vc}) with associated weight fraction ($wt_1\%$), onset temperature of PLLA degradation (T_{onset}), 80% weight loss ($T_{80\%}$), 50% weight loss ($T_{50\%}$), 30% weight loss ($T_{30\%}$) and maximum decomposition (T_{max}) with associated weight percentage ($wt_2\%$) of neat PLLA and PLLA - MOF MMMs. All PLLA - MOF samples contained around 14% volatile compounds that may primarily constitute of trapped chloroform. PLLA shows normally no degradation behavior up to temperatures around 290 - 300 °C. [53] The incorporation of MOF particles into the PLLA reduced the T_{max} suggesting that the introduction of MOF particles accelerates the thermal degradation of PLLA. It can also be assumed that the MOF particles decrease the activation energy for PLLA degradation reactions and that the difference in crystallinity of the PLLA - MOF MMMs has an impact on the PLLA degradation rate. [22, 53] The variable wt% of MOF in the samples for the different PLLA - MOF ratios indicated that the MOF particles were not well dispersed in the PLLA matrix.

Table 7: TGA analysis of neat PLLA and PLLA - MOF MMMs.

Samples	Volatile compound		PLLA				MOF	
	T _{vc} (°C)	Wt ₁ %	T _{onset} (°C)	T _{80%} (°C)	T _{50%} (°C)	T _{30%} (°C)	T _{max} (°C)	Wt ₂ %
PLLA	174.18 ± 0.61 ^A	87.53 ± 0.28 ^A	322.33 ± 0.40 ^A	334.92 ± 1.00 ^A	357.24 ± 0.89 ^A	365.39 ± 0.93 ^A	379.03 ± 0.99 ^A	-
PLLA- 1% MOF	166.66 ± 5.63 ^A	87.23 ± 0.33 ^A	312.16 ± 0.40 ^B	323.48 ± 0.47 ^B	343.28 ± 0.46 ^B	349.76 ± 0.57 ^B	358.80 ± 1.38 ^B	1.75 ± 0.56 ^A
PLLA- 5% MOF	162.59 ± 5.41 ^B	86.37 ± 0.47 ^B	302.62 ± 1.75 ^C	312.57 ± 2.14 ^C	333.19 ± 1.03 ^C	339.23 ± 1.17 ^C	347.41 ± 0.60 ^C	1.45 ± 4.75 ^A
PLLA- 10% MOF	167.47 ± 4.77 ^A	85.06 ± 0.55 ^{B,C}	302.05 ± 2.27 ^C	304.03 ± 4.47 ^D	330.60 ± 0.63 ^D	337.57 ± 0.71 ^C	346.27 ± 0.12 ^C	3.34 ± 2.47 ^A
PLLA- 20% MOF	162.03 ± 3.35 ^B	84.87 ± 0.09 ^C	295.03 ± 7.51 ^C	279.86 ± 3.62 ^E	330.36 ± 1.40 ^D	336.87 ± 1.85 ^C	347.75 ± 3.23 ^C	16.41 ± 1.99 ^B

Mean ± standard deviation followed by the same superscript in the same column are not statistically significantly different ($p > 0.05$). The '-' symbol denotes no results were obtained.

5.4 Scanning Electron Microscopy

Figure 16 shows SEM images of MOF particles and the surface of neat PLLA solvent casted samples. SEM analysis indicated that MOF particles were a cubical shape and the particle size of distribution of around 31,55 μm found in the literature was verified. [54] The neat PLLA exhibited small circular shaped irregularities derived from trapped chloroform in the samples.

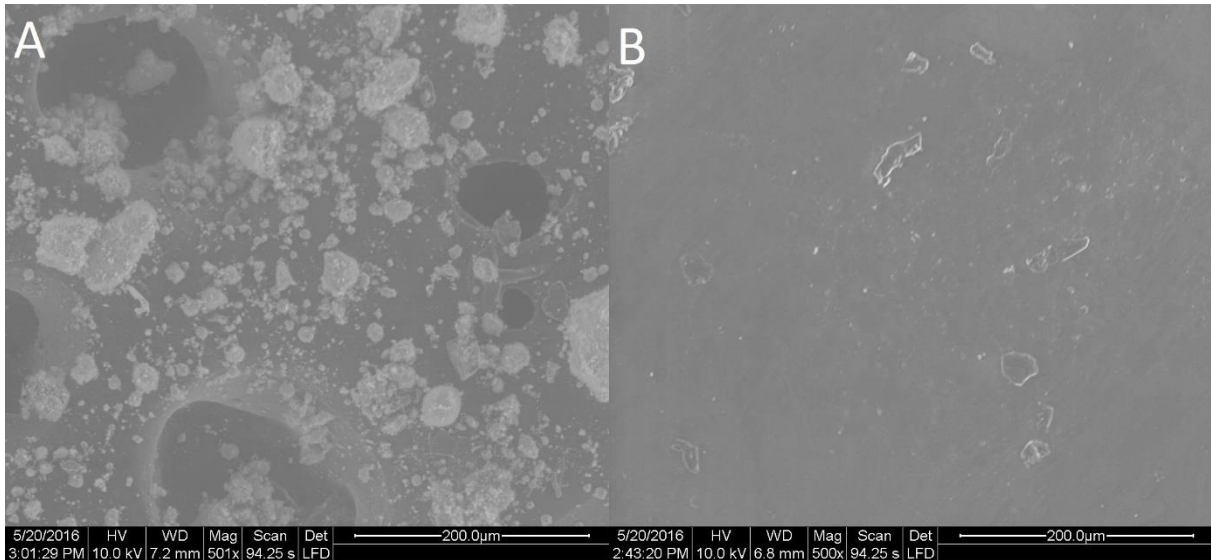


Figure 16: SEM images of MOF and neat PLLA. A: MOF magnification 500x, scale bar 200 μm ; B: neat PLLA magnification 500x, scale bar 200 μm .

Figure 17 shows the SEM images of PLLA - 1% MOF, PLLA - 5% MOF, PLLA - 10% MOF and PLLA - 20% MOF. Circular shapes derived from trapped chloroform were observed in all PLLA - MOF MMMs. The SEM analysis revealed that MOF particles have the tendency to accumulate within the PLLA matrix, resulting in a non-homogeneous dispersion.

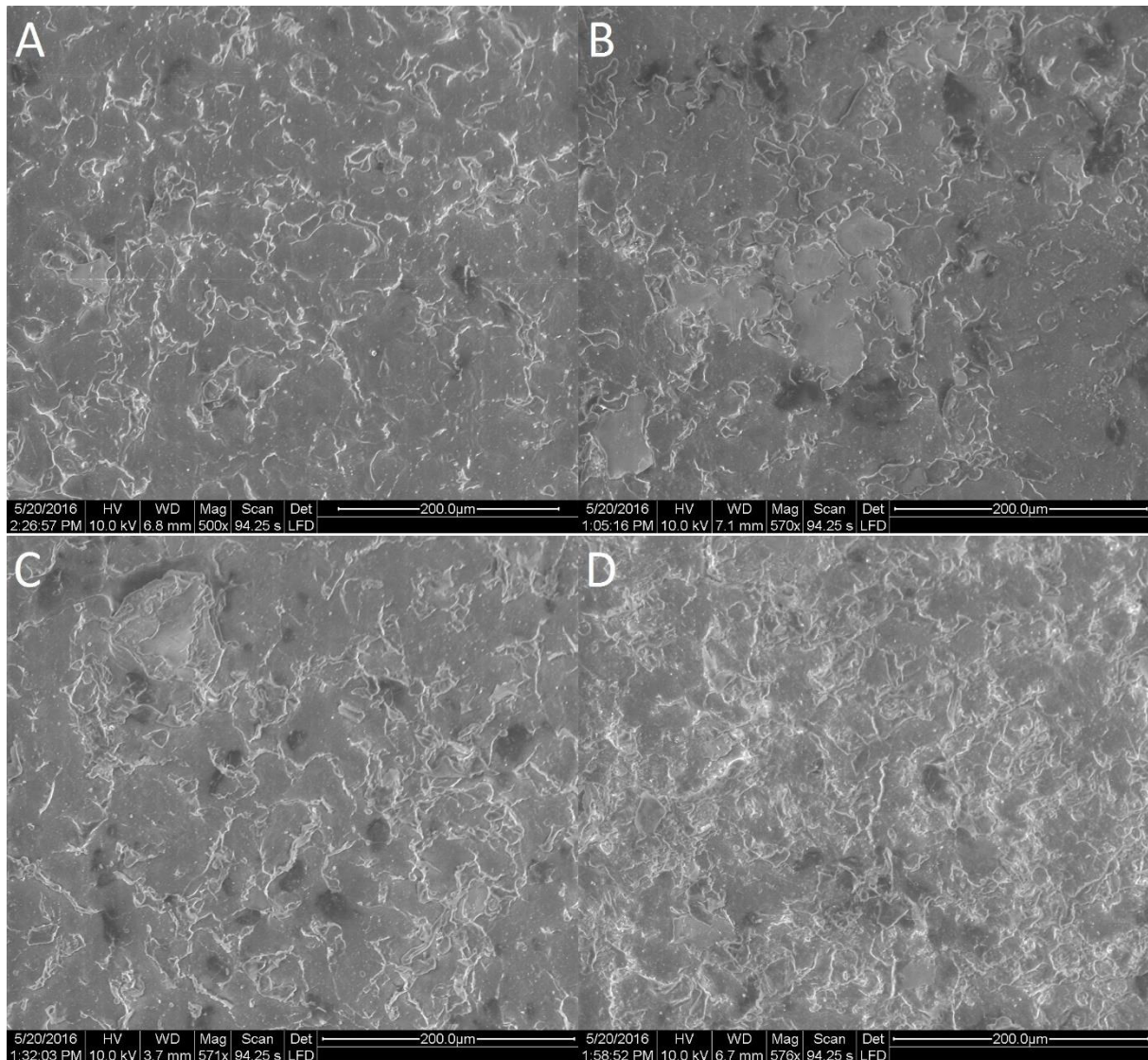


Figure 17: SEM images of PLLA - 1% MOF, PLLA - 5% MOF, PLLA - 10% MOF and PLLA - 20% MOF. A: PLLA - 1% MOF magnification: 500x, scale bar 200 µm. B: PLLA - 5% MOF magnification: 570x, scale bar 200 µm. C: PLLA - 10% MOF magnification: 571x, scale bar 200 µm. D: PLLA - 20% MOF magnification: 576x, scale bar 200 µm.

6 Conclusion

PLLA - MOF MMMs with 1, 5, 10 and 20 wt% MIL - 53 (Al) were fabricated by solvent casting and characterization was performed using fourier transform infrared spectroscopy, differential scanning calorimetry, thermogravimetric analysis and scanning electron microscopy. FTIR results showed that the presence of MOF in the PLLA - MOF spectra increased by adding more MOF to the PLLA matrix. No band shifts or new band peaks were observed by the addition of MOF suggesting that no chemical reactions occurred. The area under the peak of 923 cm^{-1} assigned to the presence of PLLA α crystals was calculated and revealed that the addition of MOF particles to the PLLA matrix resulted in a decrease in crystallinity. This phenomenon was also observed in the 2nd heating cycle of the DSC analysis. DSC results discovered that MOF particles impede the PLLA chains to crystallize. The percent crystallinity of neat PLLA was found to be 3.23 % and decreased around 4% for PLLA - 1% MOF and 85% for PLLA - 5% MOF as compared to neat PLLA while PLLA - 10% MOF and PLLA - 20% MOF were completely amorphous. TGA analysis showed that the polymer thermally decomposed more easily by addition of MOF to the PLLA matrix, suggesting that the MOF particles reacted as a depolymerization catalyst for PLLA. Another reason could be the change in crystallinity of the PLLA - MOF MMMs because crystallinity of PLLA has a negative effect on the degradation of PLLA. [22] The incorporation of MOF particles into the PLLA reduced the maximum degradation temperature signifying that the introduction of MOF particles accelerates the thermal degradation of PLLA. The variable wt% of MOF in the samples for the different PLLA - MOF ratios indicated that the MOF particles were not well dispersed in the PLLA matrix. An average of 14% volatile compound originated from trapped chloroform and water was found in neat PLLA and PLLA - MOF compounds. This was confirmed by SEM analysis where was shown that the MOF particles have the tendency to accumulate within the PLLA matrix. Trapped chloroform was observed in neat PLLA and in all PLLA - MOF MMMs. No results were obtained by permeability tests due to the existence of holes in the compression molded samples. This master's thesis contributed to better understand the fabrication method of PLLA - MOF MMMs and the effect of MOF particles on the thermal properties of these MMMs.

7 Further Improvements

To achieve more homogeneous mixed matrix membranes, the synthesis technique has to be reassessed. Other research mentioned mixing times of 24h to create more homogeneous MMMs. [55] The use of another solvent than chloroform can be investigated. Besides the solvent casting, DSM microextruder-compounder could be a viable solution to receive better dispersed MMMs. [56] The sonication can be reviewed and adjusted to increase break up particle aggregation and to enhance homogeneity. Another solution is to mix MOF particles and PLLA in chloroform separately and to prime the MOF solution. Priming means adding a small amount of the PLLA solution to the MOF solution to provide a thin polymer coating on the external surface of the MOF to prevent agglomeration. [57]

8 References

1. Siracusa, V., et al., *Biodegradable polymers for food packaging: a review*. Trends in Food Science & Technology, 2008. 19(12): p. 634-643.
2. Bohlmann, G.M., *Biodegradable packaging life-cycle assessment*. Environmental Progress, 2004. 23(4): p. 342-346.
3. Elangovan, D., *Characterization of metal organic framework and polymer composites and the method of their preparation*. 2010.
4. Gourmelon, G., *Global Plastic Production Rises, Recycling Lags*. Vital Signs, 2015: p. 7.
5. Drumright, R.E., P.R. Gruber, and D.E. Henton, *Poly(lactic acid) technology*. Advanced Materials, 2000. 12(23): p. 1841-1846.
6. Auras, R., B. Harte, and S. Selke, *An overview of polylactides as packaging materials*. Macromolecular Bioscience, 2004. 4(9): p. 835-864.
7. Bajpai, P.K., I. Singh, and J. Madaan, *Development and characterization of PLA-based green composites: A review*. Journal of Thermoplastic Composite Materials, 2014. 27(1): p. 52-81.
8. Kathuria, A., *Functional properties and stability of PLLA-Metal organic framework based mixed matrix membranes*. 2013.
9. Zornoza, B., et al., *Metal organic framework based mixed matrix membranes: An increasingly important field of research with a large application potential*. Microporous and Mesoporous Materials, 2013. 166: p. 67-78.
10. Mahajan, R. and W.J. Koros, *Mixed matrix membrane materials with glassy polymers. Part 2*. Polymer Engineering and Science, 2002. 42(7): p. 1432-1441.
11. Mahajan, R. and W.J. Koros, *Mixed matrix membrane materials with glassy polymers. Part 1*. Polymer Engineering and Science, 2002. 42(7): p. 1420-1431.
12. Kathuria, A., et al., *The Influence of Cu-3(BTC)(2) metal organic framework on the permeability and perm-selectivity of PLLA-MOF mixed matrix membranes*. Journal of Applied Polymer Science, 2015. 132(46): p. 10.
13. Sadakiyo, M., et al., *A significant change in selective adsorption behaviour for ethanol by flexibility control through the type of central metals in a metal-organic framework*. Chemical Science, 2016. 7(2): p. 1349-1356.
14. Kathuria, A., M.G. Abiad, and R. Auras, *Toughening of poly(L-lactic acid) with Cu₃BTC₂ metal organic framework crystals*. Polymer, 2013. 54(26): p. 6979-6986.
15. Liu, D.D., et al., *The structure-directed effect of Al-based metal-organic frameworks on fabrication of alumina by thermal treatment*. Materials Research Bulletin, 2015. 65: p. 287-292.
16. Gaab, M., et al., *The progression of Al-based metal-organic frameworks - From academic research to industrial production and applications*. Microporous and Mesoporous Materials, 2012. 157: p. 131-136.
17. Strnad, J., Z. Strnad, and J. Gestak, *Physico-chemical properties and healing capacity of potentially bioactive titanium surface*. Journal of Thermal Analysis and Calorimetry, 2007. 88(3): p. 775-779.
18. Averous, L., *Poly(lactic Acid): Synthesis, Structures, Properties, Processing, and Applications*. 2008.
19. Bordes, P., E. Pollet, and L. Averous, *Nano-biocomposites: Biodegradable polyester/nanoclay systems*. Progress in Polymer Science, 2009. 34(2): p. 125-155.
20. Arvanitoyannis, I.S., *Totally and partially biodegradable polymer blends based on natural and synthetic macromolecules: Preparation, physical properties, and potential as food packaging materials*. Journal of Macromolecular Science-Reviews in Macromolecular Chemistry and Physics, 1999. C39(2): p. 205-271.
21. Weber, C.J., et al., *Production and applications of biobased packaging materials for the food industry*. Food Additives and Contaminants, 2002. 19: p. 172-177.

22. Garlotta, D., *A literature review of poly(lactic acid)*. Journal of Polymers and the Environment, 2001. 9(2): p. 63-84.
23. Mutsuga, M., Y. Kawamura, and K. Tanamoto, *Migration of lactic acid, lactide and oligomers from polylactide food-contact materials*. Food Additives and Contaminants Part a-Chemistry Analysis Control Exposure & Risk Assessment, 2008. 25(10): p. 1283-1290.
24. Liu, G.M., X.Q. Zhang, and D.J. Wang, *Tailoring Crystallization: Towards High-Performance Poly(lactic acid)*. Advanced Materials, 2014. 26(40): p. 6905-6911.
25. Saeidlou, S., et al., *Poly(lactic acid) crystallization*. Progress in Polymer Science, 2012. 37(12): p. 1657-1677.
26. Drieskens, M., et al., *Structure Versus Properties Relationship of Poly(lactic acid). I. Effect of Crystallinity on Barrier Properties*. Journal of Polymer Science Part B-Polymer Physics, 2009. 47(22): p. 2247-2258.
27. Auras, R.A., et al., *Mechanical, physical, and barrier properties of poly(lactide) films*. Journal of Plastic Film & Sheeting, 2003. 19(2): p. 123-135.
28. Ma, P.M., et al., *Rapid Crystallization of Poly(lactic acid) by Using Tailor-Made Oxalamide Derivatives as Novel Soluble-Type Nucleating Agents*. Industrial & Engineering Chemistry Research, 2014. 53(32): p. 12888-12892.
29. Hassan, A., *Poly(lactic acid) Based Blends, Composites and Nanocomposites*. 2012.
30. Krikorian, V. and D.J. Pochan, *Crystallization behavior of poly(L-lactic acid) nanocomposites: Nucleation and growth probed by infrared spectroscopy*. Macromolecules, 2005. 38(15): p. 6520-6527.
31. Wang, Y.J., A.D. Price, and F. Caruso, *Nanoporous colloids: building blocks for a new generation of structured materials*. Journal of Materials Chemistry, 2009. 19(36): p. 6451-6464.
32. Kitagawa, S., R. Kitaura, and S. Noro, *Functional porous coordination polymers*. Angewandte Chemie-International Edition, 2004. 43(18): p. 2334-2375.
33. Yuzay, I.E., R. Auras, and S. Selke, *Poly(lactic acid) and Zeolite Composites Prepared by Melt Processing: Morphological and Physical-Mechanical Properties*. Journal of Applied Polymer Science, 2010. 115(4): p. 2262-2270.
34. Bendahou, D., et al., *New nanocomposite design from zeolite and poly(lactic acid)*. Industrial Crops and Products, 2015. 72: p. 107-118.
35. Zhu, L.F., et al., *Mixed matrix membranes containing MIL-53(Al) for potential application in organic solvent nanofiltration*. Rsc Advances, 2015. 5(89): p. 73068-73076.
36. Basu, S., A. Cano-Odena, and I.F.J. Vankelecom, *MOF-containing mixed-matrix membranes for CO₂/CH₄ and CO₂/N₂ binary gas mixture separations*. Separation and Purification Technology, 2011. 81(1): p. 31-40.
37. Alavi, S., *Selective Guest Docking in Metal-Organic Framework Materials*. Chemphyschem, 2010. 11(1): p. 55-57.
38. Kathuria, A., M.G. Abiad, and R. Auras, *Deterioration of metal-organic framework crystal structure during fabrication of poly(L-lactic acid) mixed-matrix membranes*. Polymer International, 2013. 62(8): p. 1144-1151.
39. Murray, L.J., M. Dinca, and J.R. Long, *Hydrogen storage in metal-organic frameworks*. Chemical Society Reviews, 2009. 38(5): p. 1294-1314.
40. Couck, S., et al., *An Amine-Functionalized MIL-53 Metal-Organic Framework with Large Separation Power for CO₂ and CH₄*. Journal of the American Chemical Society, 2009. 131(18): p. 6326-+.
41. Loiseau, T., et al., *A rationale for the large breathing of the porous aluminum terephthalate (MIL-53) upon hydration*. Chemistry-a European Journal, 2004. 10(6): p. 1373-1382.
42. Yan, J.L., et al., *Metal-organic framework MIL-53(Al): synthesis, catalytic performance for the Friedel-Crafts acylation, and reaction mechanism*. Science China-Chemistry, 2015. 58(10): p. 1544-1552.

43. Yehia, H., et al., *Methane facilitated transport using copper(II) biphenyl dicarboxylate-triethylenediamine/poly(3-acetoxyethylthiophene) mixed matrix membranes*. Abstracts of Papers of the American Chemical Society, 2004. 227: p. U351-U351.
44. Klyamkin, S.N., et al., *Composite Membranes Containing Metal-Organic Polymers: Morphology and Gas Transport Properties*. Petroleum Chemistry, 2014. 54(7): p. 482-490.
45. Quiros, J., et al., *Antimicrobial metal-organic frameworks incorporated into electrospun fibers*. Chemical Engineering Journal, 2015. 262: p. 189-197.
46. Byun, Y., et al., *The effect of solvent mixture on the properties of solvent cast polylactic acid (PLA) film*. Journal of Applied Polymer Science, 2012. 124(5): p. 3577-3582.
47. Kister, G., G. Cassanas, and M. Vert, *Effects of morphology, conformation and configuration on the IR and Raman spectra of various poly(lactic acid)s*. Polymer, 1998. 39(2): p. 267-273.
48. Kister, G., et al., *Vibrational analysis of Poly(L-lactic acid)*. Journal of Raman Spectroscopy, 1995. 26(4): p. 307-311.
49. Salazar, J.M., et al., *Characterization of adsorbed water in MIL-53(Al) by FTIR spectroscopy and ab-initio calculations*. Journal of Chemical Physics, 2015. 142(12): p. 11.
50. Hu, Y., et al., *Crystallization behavior of poly(L-lactic acid) affected by the addition of a small amount of poly(3-hydroxybutyrate)*. Polymer, 2008. 49(19): p. 4204-4210.
51. Zhang, J.M., et al., *Structural changes and crystallization dynamics of poly(L-lactide) during the cold-crystallization process investigated by infrared and two-dimensional infrared correlation spectroscopy*. Macromolecules, 2004. 37(17): p. 6433-6439.
52. Nishida, H., et al., *Selective Depolymerization and Effects of Homolysis of Poly(L-lactic acid) in a Blend with Polypropylene*. International Journal of Polymer Science, 2009: p. 9.
53. Yuzay, I.E., et al., *Effects of synthetic and natural zeolites on morphology and thermal degradation of poly(lactic acid) composites*. Polymer Degradation and Stability, 2010. 95(9): p. 1769-1777.
54. Sigma-Aldrich, *Safety Data sheet Basolite A100*, Sigma-Aldrich, Editor. 2015.
55. Dorosti, F., M. Omidkhah, and R. Abedini, *Fabrication and characterization of Matrimid/MIL-53 mixed matrix membrane for CO₂/CH₄ separation*. Chemical Engineering Research & Design, 2014. 92(11): p. 2439-2448.
56. Elangovan, D., et al., *Poly(L-lactic acid) metal organic framework composites: optical, thermal and mechanical properties*. Polymer International, 2012. 61(1): p. 30-37.
57. Hsieh, J.O., et al., *MIL-53 frameworks in mixed-matrix membranes*. Microporous and Mesoporous Materials, 2014. 196: p. 165-174.

Auteursrechtelijke overeenkomst

Ik/wij verlenen het wereldwijde auteursrecht voor de ingediende eindverhandeling:

Fabrication and Characterization of Poly (L-lactic acid) Aluminum based Metal Organic Frameworks Mixed Matrix Membranes

Richting: **master in de industriële wetenschappen: verpakkingstechnologie**

Jaar: **2016**

in alle mogelijke mediaformaten, - bestaande en in de toekomst te ontwikkelen - , aan de Universiteit Hasselt.

Niet tegenstaand deze toekenning van het auteursrecht aan de Universiteit Hasselt behoud ik als auteur het recht om de eindverhandeling, - in zijn geheel of gedeeltelijk -, vrij te reproduceren, (her)publiceren of distribueren zonder de toelating te moeten verkrijgen van de Universiteit Hasselt.

Ik bevestig dat de eindverhandeling mijn origineel werk is, en dat ik het recht heb om de rechten te verlenen die in deze overeenkomst worden beschreven. Ik verklaar tevens dat de eindverhandeling, naar mijn weten, het auteursrecht van anderen niet overtreedt.

Ik verklaar tevens dat ik voor het materiaal in de eindverhandeling dat beschermd wordt door het auteursrecht, de nodige toelatingen heb verkregen zodat ik deze ook aan de Universiteit Hasselt kan overdragen en dat dit duidelijk in de tekst en inhoud van de eindverhandeling werd genotificeerd.

Universiteit Hasselt zal mij als auteur(s) van de eindverhandeling identificeren en zal geen wijzigingen aanbrengen aan de eindverhandeling, uitgezonderd deze toegelaten door deze overeenkomst.

Voor akkoord,

Brouwers, Niels

Datum: **6/06/2016**